ADVANCED SUPERCONDUCTING MAGNETS INVESTIGATION

Frank Di Salvo

Third Quarterly Progress Report

AVCO EVERETT RESEARCH LABORATORY
a division of
AVCO CORPORATION
Everett, Massachusetts

10 May 1967 through 10 August 1967

Contract NAS 8-21037

prepared for

GEORGE C. MARSHALL SPACE FLIGHT CENTER
NATIONAL AERONAUTICS AND SPACE ADMINISTRATION
Huntsville, Alabama

TABLE OF CONTENTS

I. INTRODUCTION

During the last quarter, further analytical work has been done concerning the effects of the non-linear heat transfer characteristic of helium on the terminal characteristics of a composite conductor. In Section II, the one dimensional model discussed in the second quarterly report[1] is completed; it is shown from this that a better model of the heat transfer characteristics is needed to obtain results that agree with experiment. This model is introduced, and a complete solution to the one dimensional problem is given in Section III.

Many experiments have been carried out on both short samples and a large coil. Section IV deals with the results and a comparison of these results with the one dimensional theory. The data from the large coil shows two and three dimensional effects that are reasonably easy to understand and helps suggest a proper model for which two and three dimensional solutions should be obtained.

In past analyses, we have assumed that the current in the superconductor is just the critical current at the composite conductor temperature. Recent experimental evidence[2] shows that this is not exactly the case; thus a more sophisticated model of the superconductor is introduced in Section V. It is shown, by comparison with experiment, that the former model of the superconductor is sufficient to explain experimental results; even though the latter model is "more correct."

Finally, an errata is included to correct some small errors in the First Quarterly Report.

Note:

Throughout this report we will refer to:

1. The First Quarterly Progress Report[3] as 1st QPR
2. The Second Quarterly Progress Report[1] as 2nd QPR
3. The Third Quarterly Progress Report as 3rd QPR

II. COMPOSITE SUPERCONDUCTOR BEHAVIOR INCLUDING TEMPERATURE GRADIENTS ALONG WITH CONDUCTOR AND INCORPORATING THE NON-LINEAR HEAT TRANSFER CHARACTERISTIC USED IN 2nd QPR

In the 2nd QPR a one dimensional solution is obtained assuming the heat transfer characteristic of helium to be approximated by the curve shown in Fig. 1. This solution is to the problem of an external heat input at the origin of an infinitely long "wire". The wire is assumed to be thin enough so that the temperature over any given cross section, normal to the current flow, is uniform. Thus, the heat flow inside the conductor is one dimensional and in the same direction (parallel or anti-parallel) as the current flow.

A solution is obtained for the assumptions: 1) $1 - \tau > \theta_m$ and 2) the non-dimensional temperature at the origin θ_o is less than one, so that the current is shared between the substrate and superconductor at the origin. If we do not make the assumption that $\theta_m = Q_m$ as on page 19 of the 2nd QPR, we find that:

i) If $\alpha \tau^2 > Q_m$, then a sudden take off in voltage is obtained as the heat input to the origin is increased. At the take-off heat input, assumption 1 and 2 above are satisfied; thus, the solution is valid.

ii) If $\alpha \tau^2 < Q_m$ at the calculated take-off heat input, the non-dimensional temperature at the origin is greater than one. Thus, assumption 2 is not valid. We conclude, then, that for θ_o less than one, take off can not occur when $\alpha \tau^2 < Q_m$.

It is now necessary to find the solution for the case that $\theta_o > 1$, then at the origin all the current is in the substrate.

This solution will answer the questions: 1) when $\alpha \tau^2 > Q_m$ is there any hysteresis or at take off does the voltage go to infinity? 2) When $\alpha \tau^2 < Q_m$ does the conductor ever reach a "take-off" condition as the heat input at the origin is increased?

The case to be solved is shown in Fig. 2 (This is the same as is shown in Fig. 4 of the 2nd QPR).*

The equations to be satisfied in the various regions are:

*Note that the nomenclature has been changed somewhat. In the 2nd QPR Δx is the length of the shared region. We will adopt the convention that Δx is the distance from the origin to the end of the shared region.

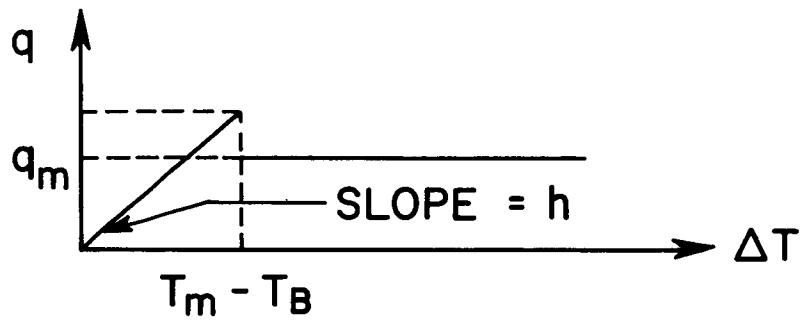

OR IN NON-DIMENSIONAL NOTATION

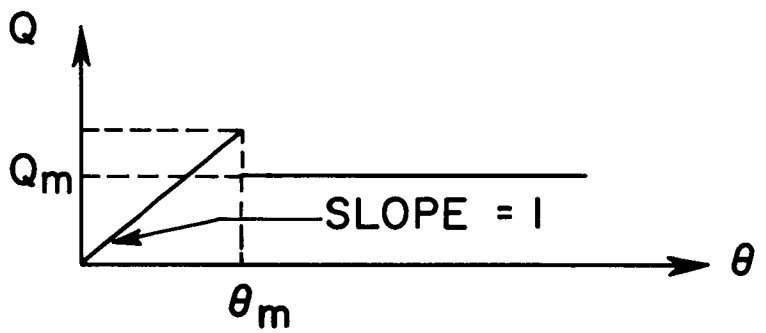

Fig. 1 The first non-linear model for the heat transfer characteristics of liquid helium

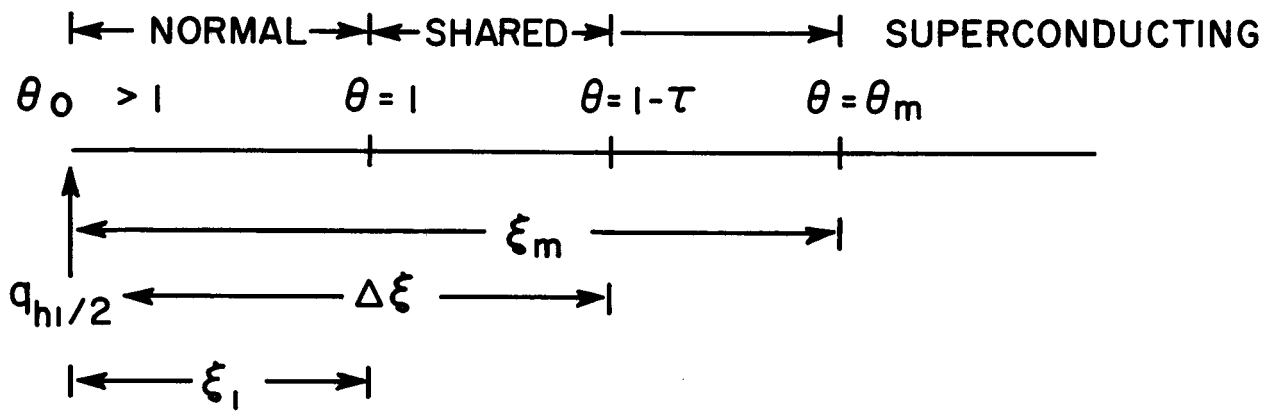

Fig. 2 A schematic of the regions present when Θ (o) > 1 for a composite superconductor

REGION	SHARING CONDITION	EQUATION
$0 < \xi < \xi_1$	$f = 1$	$\frac{d^2\Theta}{d\xi^2} - Q_m + \alpha\tau^2 = 0$ (1)
$\xi_1 < \xi < \Delta\xi$	$0 < f < 1$	$\frac{d^2\Theta}{d\xi^2} - Q_m + \alpha\tau(\tau - 1 + \Theta) = 0$ (2)
$\Delta\xi < \xi < \xi_m$	$f = 0$	$\frac{d^2\Theta}{d\xi^2} - Q_m = 0$ (3)
$\xi > \xi_m$	$f = 0$	$\frac{d^2\Theta}{d\xi^2} - \Theta = 0$ (4)

where we assume $1 - \tau > \Theta_m$.

The parameters Θ, Q_m, α, τ, f, ξ have been defined in the 1st and 2nd QPR. The solutions to these equations are:

$0 < \xi < \xi_1$, $\Theta = 1/2\,(Q_m - \alpha\tau^2)\,\xi^2 + C_1\xi + C_2$ (5)

$\xi_1 < \xi < \Delta\xi$, $\Theta = C_3 \sin\sqrt{\alpha\tau}\,\xi + C_4 \cos\sqrt{\alpha\tau}\,\xi + \frac{Q_m}{\alpha\tau} + 1 - \tau$ (6)

$\Delta\xi < \xi < \xi_m$, $\Theta = 1/2\,Q_m\,\xi^2 + C_5\,\xi + C_6$ (7)

$\xi > \xi_m$, $\Theta = C_7\,e^{-\xi} + C_8 e^{+\xi}$ (8)

The boundary conditions are:

i) $\Theta \to 0$ as $\xi \to \infty$

ii) $\left.\frac{d\Theta}{d\xi}\right|_{\xi = 0} = -Q_{h1}$

Q_{h1} has been defined in the 2nd QPR

iii) Θ and $\frac{d\Theta}{d\xi}$ are continuous at $\xi = \xi_1,\ \Delta\xi,\ \xi_m$.

The boundary conditions completely determine the constants C_1 thru C_8 as well as the lengths ξ_1, $\Delta\xi$, and ξ_m.

The constants are determined* to be:

$$C_1 = - Q_{h1}$$

$$C_2 = 1 - 1/2 \, (Q_m - a\tau^2) \, \xi_1^2 + Q_{h1} \, \xi_1$$

$$C_3 = - \frac{Q_m}{a\tau} \sin \sqrt{a\tau} \; \Delta\xi - \frac{Q_m}{\sqrt{a\tau}} \sqrt{\frac{\theta_m^2}{Q_m^2} + \frac{2}{Q_m} (1 - \tau - \theta_m)} \cos \sqrt{a\tau} \; \Delta\xi$$

$$C_4 = \frac{Q_m}{\sqrt{a\tau}} \sqrt{\frac{\theta_m^2}{Q_m^2} + \frac{2}{Q_m} (1 - \tau - \theta_m)} \sin \sqrt{a\tau} \; \Delta\xi - \frac{Q_m}{a\tau} \cos \sqrt{a\tau} \; \Delta\xi$$

$$C_5 = - (\theta_m + Q_m \, \xi_m)$$

$$C_6 = (\theta_m + Q_m \, \xi_m) \, \xi_m - 1/2 \, Q_m \, \xi_m^2 + \theta_m$$

$$C_7 = \theta_m \, e^{\xi_m}$$

$$C_8 = 0$$

The non-dimensional lengths are determined by the following equations:

$$\xi_m - \Delta\xi = - \frac{\theta_m}{Q_m} + \sqrt{\frac{\theta_m}{Q_m^2} + \frac{2}{Q_m} (1 - \tau - \theta_m)} \tag{9}$$

$$\tau - \frac{Q_m}{a\tau} = \frac{Q_m}{\sqrt{a\tau}} \sqrt{\frac{\theta_m^2}{Q_m^2} + \frac{2}{Q_m} (1 - \tau - \theta_m)} \sin \sqrt{a\tau} \, (\Delta\xi - \xi_1) - \frac{Q_m}{a\tau} \cos \sqrt{a\tau} \; (\Delta\xi - \xi_1) \tag{10}$$

*Note: The algebraic form of the constants depends upon which of the eleven boundary conditions are used to determine them; however, in any specific case the numerical values of the constants are independent of the boundary conditions used, as they should be.

$$Q_{h1} = (Q_m - a\tau^2)\,\xi_1 + \frac{Q_m}{\sqrt{a\tau}} \sin \sqrt{a\tau}\,(\Delta\xi - \xi_1) + Q_m\sqrt{\frac{\theta_m^2}{Q_m^2} + \frac{2}{Q_m}(1 - \tau - \theta_m)}\times$$

$$\cos \sqrt{a\tau}\,(\Delta\xi - \xi_1) \qquad (11)$$

Note from Eq. (9) that $(\xi_m - \Delta\xi)$, the length of the fully superconducting region that is film boiling, and from Eq. (10) $(\Delta\xi - \xi_1)$, the length of the shared region, are independent of Q_{h1}, the non-dimensional heat input at the origin. From Eq. (11), only ξ_1, the length of the normal region is affected by Q_{h1}. Equation (10) has a solution only if the maximum value of the right hand side of the equation is greater than the left hand side of the equation. It is easily found that this condition is satisfied if:

$$\theta_m^2 + 2\,Q_m\,(1 - \theta_m) - a\tau^3 > 0 \qquad (12)$$

It is easy to show that this condition always holds if $Q_m > a\tau^2$ by replacing $a\tau^3$ by $2\tau\,Q_m$ (which is larger than $a\tau^3$ by the condition $Q_m > a\tau^2$). Then Eq. (13) becomes:

$$\theta_m^2 + 2\,Q_m\,(1 - \tau - \theta_m) > 0$$

But this is always true since we have found the solution for the assumption $1 - \tau > \theta_m$. It is obvious from the above method that Eq. (13) will also hold if $a\tau^2$ is not too much greater than Q_m. If Eq. (12) is not satisfied, then a solution to the problem with the given boundary conditions ($\theta = 0$ as $\xi \to \infty$) is not possible.

If $a\tau^2 > Q_m$ and condition 12 is not satisfied; then the voltage takes off as a heat input of

$$Q_{h1T} = \sqrt{\frac{Q_m^2}{a\tau} + \theta_m^2 + 2\,Q_m\,(1 - \tau - \theta_m)} \qquad (13)$$

which is obtained from the analysis presented in the 2nd QPR, without assuming $\theta_m = Q_m$. At take-off the voltage increases to infinity and the wire "quenches."

Assuming that Eq. (12) is satisfied, we obtain from Eq. (11)

$$\frac{dQ_{h1}}{d\,\xi_1} = (Q_m - a\tau^2)$$

since the length of the shared region $(\Delta\xi - \xi_1)$, is independent of the length of the normal region, ξ_1. Now $\frac{dV}{dQ_{h1}}$ (V is the conductor voltage) must be

positive and finite for stable operation to occur and consequently $\frac{dQ_{hl}}{dV} = \frac{d\,Q_{hl}}{d\,\xi_1} \cdot \frac{d\,\xi_1}{d\,V}$ must be positive. Then $\frac{dQ_{hl}}{d\,\xi_1}$ must be positive and finite since $d\,\xi_1/dV$ is always positive. Thus if

1) $Q_m > a\,\tau^2$ stable operation always occurs independent of how much heat is added at the origin.

2) $Q_m < a\,\tau^2$ the voltage takes off at a value given by Eq. (13) and it goes to infinity.

We conclude then, that with this model of the heat transfer characteristic, the wire is either stable or unstable with NO HYSTERESIS REGION between.

Experimentally a region of hysteresis is always observed; so we must choose a model for the heat transfer characteristic which corresponds more closely to the real case. We choose that characteristic to be as shown in Fig. 3.

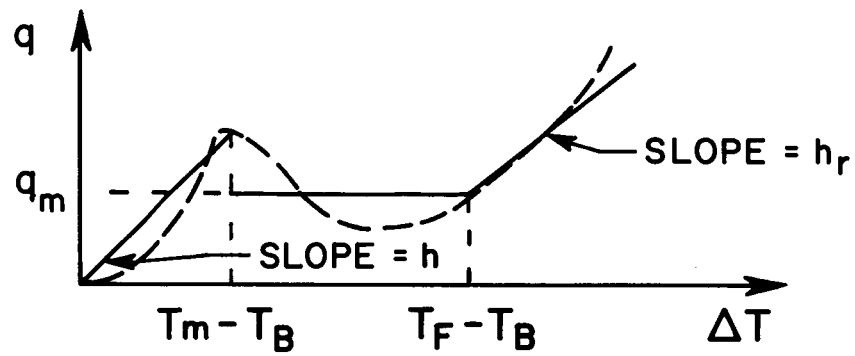

OR IN NON-DIMENSIONAL FORM

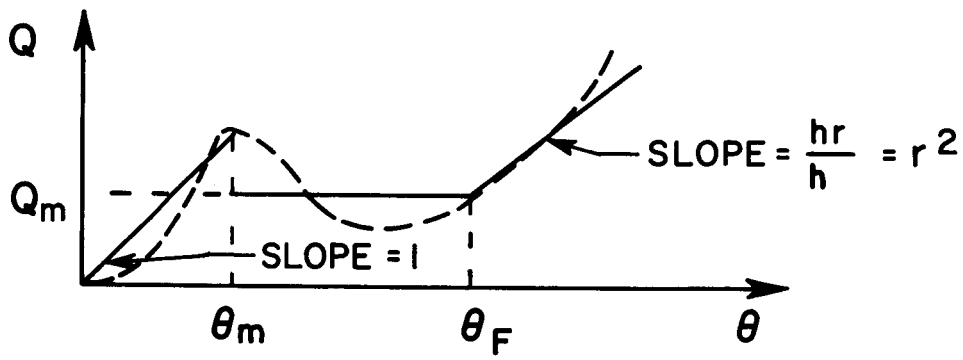

Fig. 3 Second non-linear model for the heat transfer characteristic of liquid helium

III. COMPOSITE SUPERCONDUCTOR BEHAVIOR INCLUDING TEMPERATURE GRADIENTS ALONG THE CONDUCTOR AND INCORPORATING A NEW NON-LINEAR HEAT TRANSFER CHARACTERISTIC

The heat transfer characteristic that we will now use is shown in Fig. 3. This will be called the 2nd non-linear characteristic. The one used previously will be called the 1st non-linear characteristic. We have introduced some new parameters which are:

T_F = the temperature at which the heat transfer characteristic begins to rise again.

h_r = Slope of the second rise in the heat transfer characteristic.

$r^2 = \frac{hr}{h}$ = ratio of the second slope to the initial slope.

From the actual measured heat transfer characteristics we find that $T_F > T_c$ for Nb-Ti or Nb-Zr and that $r^2 < 1$. For comparison an actual heat transfer characteristic is also shown in Fig. 3 as a dotted line.

In the following analysis we will again use the same reduced variables as in the 1st and 2nd QPR. The only new variables introduced are:

$$\Theta_F = \frac{T_F - T_B}{T_C - T_B}$$

$$r^2 = \frac{hr}{h} \text{ (defined above)}$$

and ξ_F = length of normal region whose temperature is greater than T_F. Again we find the solution for the case $1 - \tau > \Theta_m$. Thus, we have that $\Theta_m < 1 - \tau < 1 < \Theta_F$.

In Fig. 4, the sequence of events as the heat input to the origin is increased from zero is shown. We indicate with each example which solution of those already worked out and the one to be worked out applies, and in which report that solution is discussed.

The case in Fig. 4 that remains unsolved is that shown in 4e. The solution follows.

The equations for the non-dimensional temperature that need to be solved are:

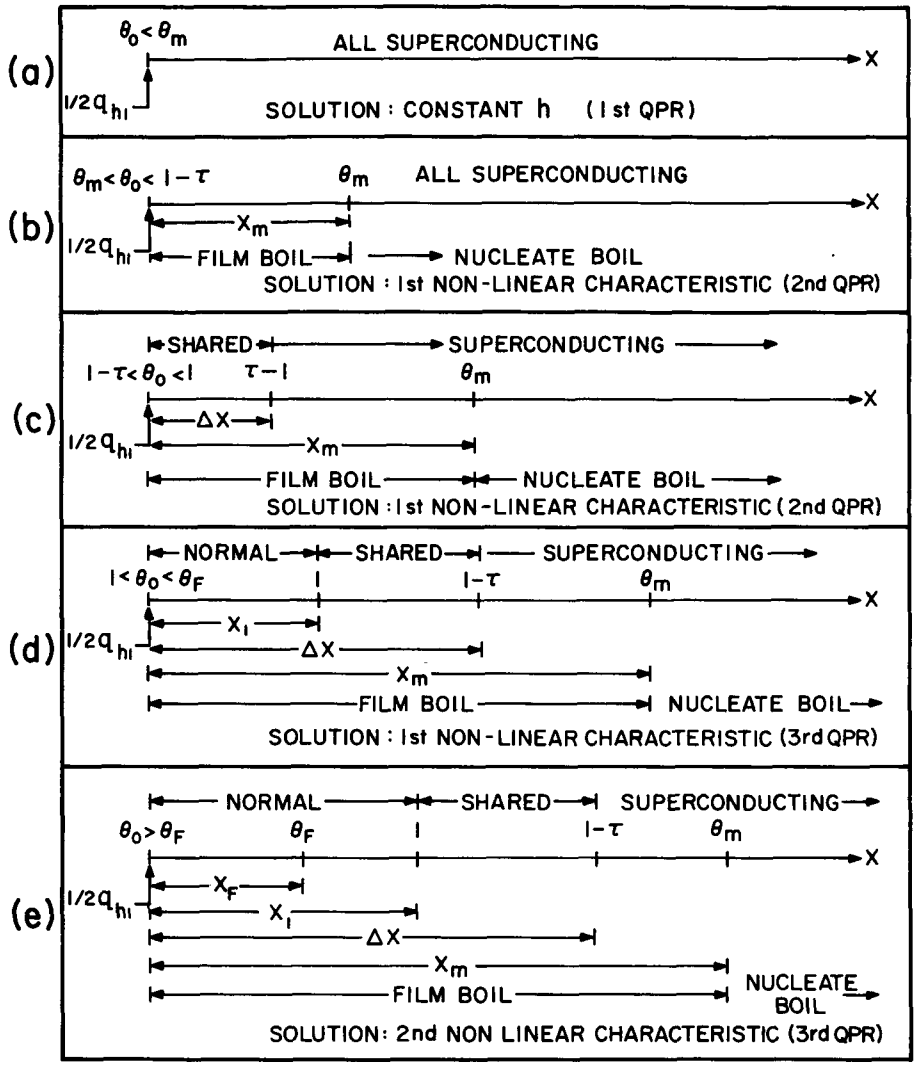

Fig. 4a Conductor cooled entirely by nucleate boiling

4b Conductor cooled partially by nucleate boiling and partially by film boiling

4c Cooling after the onset of resistance but before all of the current transfers into the substrate at the origin

4d Cooling when all the current is in the substrate at the origin but $\Theta_o < \Theta_F$

4e Cooling when $\Theta_o > \Theta_F$

REGION	SHARING CONDITION	EQUATION
$0 < \xi < \xi_F$	$f = 1$	$\frac{d^2\Theta}{d\xi^2} + \alpha\tau^2 - r^2(\Theta - \Theta_F) - Q_m = 0$ (14)
$\xi_F < \xi < \xi_1$	$f = 1$	$\frac{d^2\Theta}{d\xi^2} - Q_m + \alpha\tau^2 = 0$ (15)
$\xi_1 < \xi < \Delta\xi$	$0 < f < 1$	$\frac{d^2\Theta}{d\xi^2} - Q_m + \alpha\tau(\tau - 1 + \Theta) = 0$ (16)
$\Delta\xi < \xi < \xi_m$	$f = 0$	$\frac{d^2\Theta}{d\xi^2} - Q_m = 0$ (17)
$\xi > \xi_m$	$f = 0$	$\frac{d^2\Theta}{d\xi^2} - \Theta = 0$ (18)

The solutions to these equations are:

$0 < \xi < \xi_F$, $\Theta = C_1 \sinh r\xi + C_2 \cosh r\xi + \frac{\alpha\tau^2 - Q_m + r^2\Theta_F}{r^2}$ (19)

$\xi_F < \xi < \xi_1$, $\Theta = 1/2\ (Q_m - \alpha\tau^2)\ \xi^2 + C_3\xi + C_4$ (20)

$\xi_1 < \xi < \Delta\xi$, $\Theta = C_5 \sin\sqrt{\alpha\tau}\ \xi + C_6 \cos\sqrt{\alpha\tau}\ \xi + \frac{Q_m}{\alpha\tau} + 1 - \tau$ (21)

$\Delta\xi < \xi < \xi_m$, $\Theta = 1/2\ Q_m\ \xi^2 + C_7\ \xi + C_8$ (22)

$\xi > \xi_m$, $\Theta = C_9\ e^{-\xi} + C_{10} e^{\xi}$ (23)

Again the boundary conditions are:

i) $\Theta \to 0$ as $\xi \to \infty$

ii) $\left.\frac{d\Theta}{d\xi}\right|_{\xi = 0} = - Q_{h\,1}$

iii) Θ and $\frac{d\Theta}{d\xi}$ are continuous at $\xi = \xi_F,\ \xi_1,\ \Delta\xi,\ \xi_m$.

These conditions are sufficient to determine all the constants in the solutions and the lengths ξ_F, ξ_1, $\Delta\xi$, and ξ_m.

The constants determined from the boundary conditions are:

$$C_1 = -\frac{Q_{h1}}{r}$$

$$C_2 = \frac{\frac{Q_{h1}}{r} \sinh r\,\xi_F + \frac{Q_m - a\tau^2}{r^2}}{\cosh r\,\xi_F}$$

$$C_3 = -\sqrt{\theta_m^2 + 2\,Q_m\,(1 - \theta_m) - a\tau^3} + (a\tau^2 - Q_m)\,\xi_1$$

$$C_4 = 1 + 1/2\,(Q_m - a\tau^2)\,\xi_1^2 + \sqrt{\theta_m^2 + 2\,Q_m\,(1 - \theta_m) - a\tau^3}\,\xi_1$$

$$C_5 = -\frac{Q_m}{a\tau} \sin\sqrt{a\tau}\,\Delta\xi - \frac{Q_m}{\sqrt{a\tau}} \sqrt{\frac{\theta_m^2}{Q_m^2} + \frac{2}{Q_m}\,(1 - \tau - \theta_m)} \cos\sqrt{a\tau}\,\Delta\xi$$

$$C_6 = \frac{Q_m}{\sqrt{a\tau}} \sqrt{\frac{\theta_m^2}{Q_m^2} + \frac{2}{Q_m}\,(1 - \tau - \theta_m)} \sin\sqrt{a\tau}\,\Delta\xi - \frac{Q_m}{a\tau} \cos\sqrt{a\tau}\,\Delta\xi$$

$$C_7 = -(\theta_m + Q_m\,\xi_m)$$

$$C_8 = (\theta_m + Q_m\,\xi_m)\,\xi_m - 1/2\,Q_m\,\xi_m^2 + \theta_m$$

$$C_9 = \theta_m\,e^{\xi_m}$$

$$C_{10} = 0$$

The lengths ξ_F, ξ_1, $\Delta\xi$, ξ_m are determined using the following equations:

$$\xi_m - \Delta\xi = -\frac{\theta_m}{Q_m} + \sqrt{\frac{\theta_m^2}{Q_m^2} + \frac{2}{Q_m}\,(1 - \tau - \theta_m)} \qquad (24)$$

$$\tau - \frac{Q_m}{a\tau} = \frac{Q_m}{\sqrt{a\tau}} \sqrt{\frac{\theta_m^2}{Q_m^2} + \frac{2}{Q_m}(1 - \tau - \theta_m)} \sin \sqrt{a\tau}\,(\Delta\xi - \xi_1) - \frac{Q_m}{a\tau} \cos$$

$$\sqrt{a\tau}\,(\Delta\xi - \xi_1) \qquad (25)$$

$$\xi_1 - \xi_F = - \frac{\sqrt{\theta_m^2 + 2Q_m(1 - \theta_m) - a\tau^3}}{Q_m - a\tau^2}$$

$$+ \sqrt{\frac{\theta_m^2 + 2Q_m(\theta_F - \theta_m) - 2a\tau^2(\theta_F - 1) - a\tau^3}{(Q_m - a\tau^2)^2}} \qquad (26)$$

$$Q_{h1} \cosh r\xi_F - \left(\frac{Q_{h1}}{r} \sinh r\xi_F + \frac{Q_m - a\tau^2}{r^2}\right) r \tanh r\xi_F =$$

$$\sqrt{\theta_m^2 + 2Q_m(\theta_F - \theta_m) - 2a\tau^2(\theta_F - 1) - a\tau^3} \qquad (27)$$

Note that Eqs. (24), (25) are identical with (9), (10) of this same report. Everything previously said about Eqs. (9), (10) applies here also. The length $(\xi_1 - \xi_F)$ given by Eq. (26) does not depend on the heat input Q_{h1}. Only the length ξ_F depends on Q_{h1}. Equation (27) has a real solution only if the quantity under the radical is greater than zero. Thus the parameters must satisfy the condition:

$$\theta_m^2 + 2Q_m(\theta_F - \theta_m) - 2a\tau^2(\theta_F - 1) - a\tau^3 \geq 0 \qquad (28)$$

This condition is always satisfied if $Q_m > a\tau^2$, and is satisfied if $a\tau^2$ is not too much greater than Q_m.

If either Eq. (13) or (28) are not satisfied, then at take-off the normal region grows to infinity. Assuming that both Eqs. (12) and (28) are satisfied, we must have for stability, as before:

$$\frac{dQ_{h1}}{d\xi_F} > 0 \text{ but infinite}$$

From Eq. (27) we find:

$$\frac{dQ_{h1}}{d\xi_F} = \frac{Q_m - a\tau^2 + rQ_{h1} \sinh r\xi_F}{\cosh r\xi_F} \qquad (29)$$

Using Eq. (27) again to eliminate $Q_{h\,1}$ from Eq. (29):

$$\frac{dQ_{h\,1}}{d\,\xi_F} = (Q_m - \alpha\tau^2)\cosh r\,\xi_F + r\sqrt{\theta_m^2 + 2\,Q_m(\theta_F - \theta_m) - 2\,\alpha\tau^2(\theta_F - 1) - \alpha\tau^3}\,\sinh r\,\xi_F \quad (30)$$

In order to understand the behavior of the conductor, it is helpful to plot $Q_{h\,1}$ vs ξ_F as in Fig. 5. The heat input at the origin when $\xi_F = 0$ is determined from Eq. (27) to be:

$$Q_{h\,1}(\xi_F = 0) = \sqrt{\theta_m^2 + 2\,Q_m(\theta_F - \theta_m) - 2\,\alpha\tau^2(\theta_F - 1) - \alpha\tau^3} \quad (31)$$

which decreases for increasing τ . If $Q_m > \alpha\tau^2$, $\frac{dQ_{h\,1}}{d\,\xi_F} > 0$ for all ξ_F and the operation is stable (curve #1 - Fig. 5). If $Q_m < \alpha\tau^2$, there are two modes of behavior:

1) $\alpha\tau^2$ not much larger than Q_m (see curve #3 -- Fig. 5) the slope $\frac{dQ_{h\,1}}{d\,\xi_F}$ is negative at $\xi_F = 0$, but the curve reaches a minima and from then on the slope is positive. This change in slope must occur at a point where $Q_{h1} > 0$ (see Eq. (29))

2) $\frac{dQ_{h\,1}}{d\,\xi_F} < 0$ always (curve 4 -- Fig. 5)

From Eq. (30) we see that the plot may have minima (if $Q_m < \alpha\tau^2$) but never has a maxima for finite ξ_F. Thus take-off never occurs in this region because take-off occurs at a maxima (recovery occurs at a minima). We have shown, then, that theconductor may only take-off when in the state shown in Fig. 4 c, and if $\alpha\tau^2 > Q_m$. Thus, if $Q_m > \alpha\tau^2$, the conductor voltage vs heater power is continuous and reversible for all values of heat input at the origin.

It is easy to show that the heat input at take-off

$$Q_{h\,1\,T} > Q_{h\,1}(\xi_F = 0) \text{ if } \alpha\tau^2 > Q_m, \text{ where } Q_{h\,1\,T}$$

is found in the 2nd QPR and given in Eq. (13). At take-off, if $\alpha\tau^2$ is not much larger than Q_m (curve #3 -- Fig. 5) the normal region will grow spontaneously until ξ_F is large enough so that $Q_{h\,1\,T} = Q_{h\,1}(\xi_F)$. A further

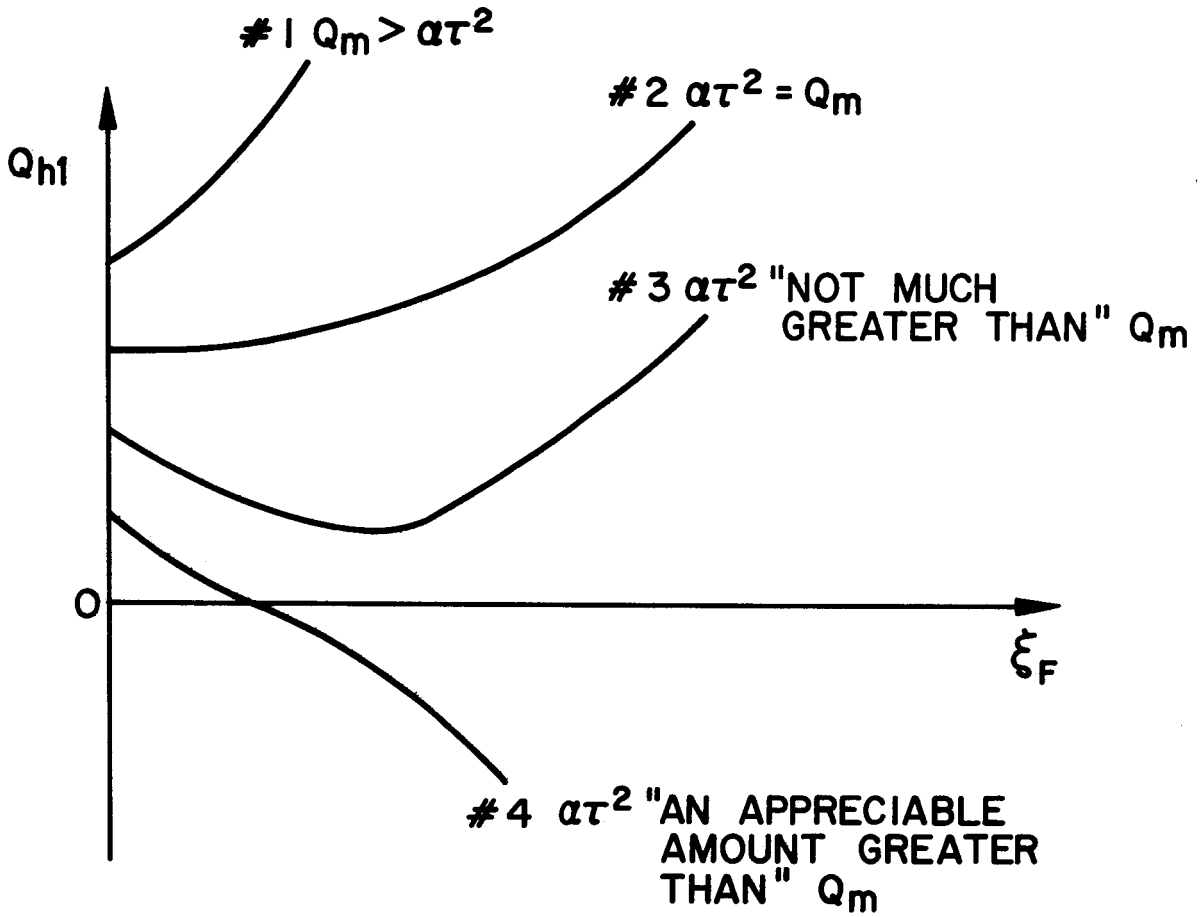

Fig. 5 A schematic of the behavior of the reduced heat input at the origin Q_n, vs the reduced length ξ_F at constant α and Q_m for different τ

increase in heat input results in a controllable voltage increase. If the heat input is reduced, recovery will occur at the minima in the $Q_{h\,1}$ vs ξ_F curve. The situation described above is called hysteresis, and the range of τ for which this occurs is called the hysteresis region.

If τ is such that the situation shown by curve 4 -- Fig. 5 exists, or if Eq. (12) or (28) is not satisfied, the wire will "quench" (develop an infinite voltage) at take-off. A schematic of typical V-Q plots (conductor voltage vs heat input) for some α and different τ is shown in Fig. 6.

The hysteresis region is determined using the fact that $\frac{dQ_{h\,1}}{d\,\xi_F}$ goes to zero only in this region. The slope is zero when (from Eq. (30))

$$\tanh r\,\xi_F = \frac{\alpha\,\tau^2 - Q_m}{r\,\sqrt{\theta_m^2 + 2\,Q_m\,(\theta_F - \theta_m) - 2\,\alpha\,\tau^2\,(\theta_F - 1) - \alpha\,\tau^3}} \qquad (32)$$

For a solution to Eq. (32) to exist with $\xi_F > 0$ we must have:

$$\alpha\,\tau^2 \geq Q_m$$

and

$$r\,\sqrt{\theta_m^2 + 2\,Q_m\,(\theta_F - \theta_m) - 2\,\alpha\,\tau^2\,(\theta_F - 1) - \alpha\,\tau^3} \leq \alpha\,\tau^2 - Q_m$$

thus the region of hysteresis is defined by:

$$Q_m < \alpha\,\tau^2 < Q_m + r\,\sqrt{\theta_m^2 + 2\,Q_m\,(\theta_F - \theta_m) - 2\,\alpha\,\tau^2\,(\theta_F - 1) - \alpha\,\tau^3} \qquad (33)$$

The last detail of the V-Q plot to be determined is the slope $\frac{dV}{dQ_{h\,1}}$ at the onset of voltage (resistance). This may be determined using the analysis presented in the 2nd QPR, since at the onset of resistance $\theta_0 = 1 - \tau < 1$. The voltage per unit length in the shared state is:

$$v = \frac{\rho I}{A}\,f = \frac{\rho I_c}{A}\,(\tau - 1 + \theta) \qquad (34)$$

Since we wish to find the solution as $\Delta\xi \to 0$ we have to lowest order in ξ and $\Delta\xi$ from Eq. (26) or 2nd QPR

$$\theta \simeq Q_{h\,1}\,(\Delta\xi - \xi) + 1 - \tau \qquad (35)$$

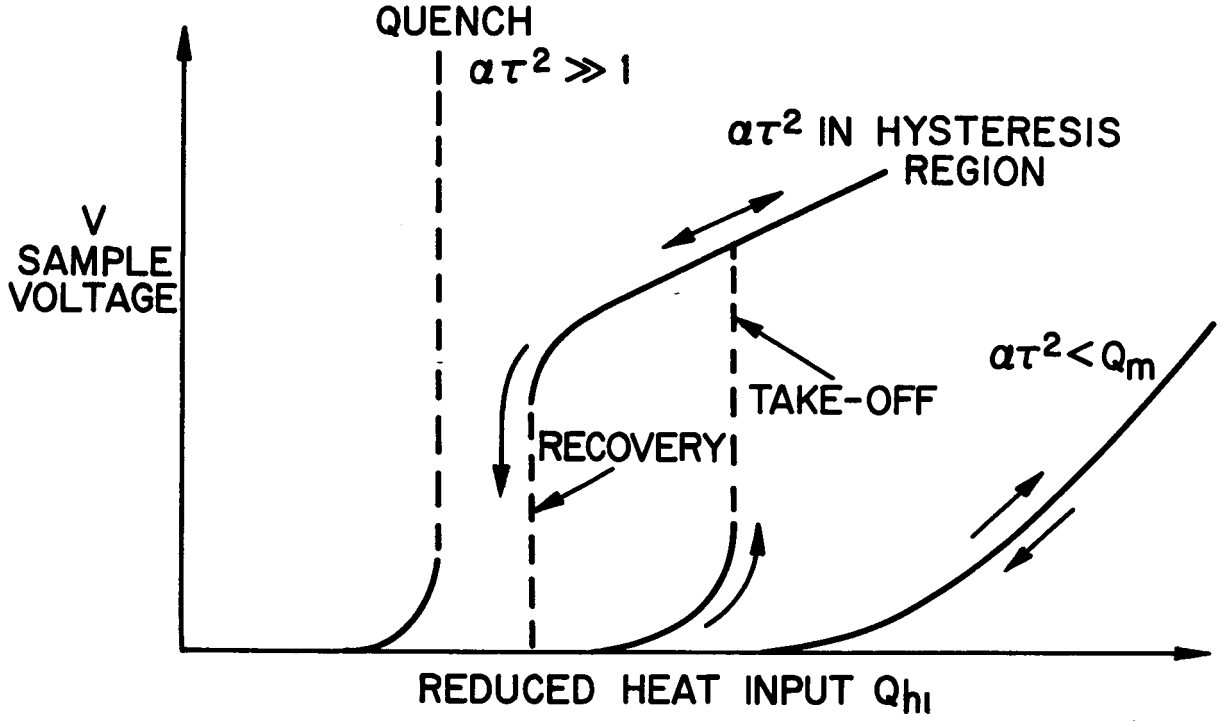

Fig. 6 Types of V-Q plots expected for a one dimensional composite superconductor at constant applied magnetic fields for different τ.

The total voltage across the conductor is:

$$V = 2 \int_0^{\Delta x} v \, dx = 2 x_o \int_0^{\Delta \xi} v \, d\xi \tag{36}$$

Using Eqs. (34) and (35), Eq. (36) becomes:

$$V = \frac{\rho I_c x_o}{A} Q_{h1} \Delta \xi^2 \tag{37}$$

At the onset of resistance $Q_{h1} = Q_{h1}\Big|_{or}$ (defined in the 2nd QPR Eqs. (31) and (32)) and $\Delta\xi = 0$. Thus the slope $\frac{dV}{dQ_{h1}}$, obtained from Eq. (37) is:

$$\frac{dV}{dQ_{h1}}\Bigg|_{Q_{h1} = Q_{h1}|_{or}} = \frac{\rho I_c x_o}{A} \left[\Delta\xi^2 + 2 Q_{h1} \Delta\xi \frac{d\Delta\xi}{d Q_{h1}}\right]$$

But, from Eq. (29) of the 2nd QPR $d\Delta\xi/dQ_{h1}$ is finite at this point and we have:

$$\frac{dV}{dQ_{h1}}\Bigg|_{Q_{h1} = Q_{h1}|_{or}} = 0 \tag{38}$$

The slope $\frac{dV}{dQ_{h1}}$ is always zero at the onset of resistance.

Recapitulating the results for the one dimensional model, with our assumption that $\Theta_m \leq 1 - \tau \leq 1 \leq \Theta_F$, we have found the heater characteristics to be:

1) the onset of resistance (or voltage) occurs at a heat input of

$$Q_{h1}\Big|_{or} = \sqrt{\Theta_m \left[2(1 - \tau) - \Theta_m\right]}$$

Eq. (31) -- 2nd QPR

2) the slope $\frac{dV}{dQ_{h1}}$ at the onset is zero.

3) If $Q_m > a\tau^2$, increasing the heat input from $Q_{h1}\Big|_{or}$ causes a controllable and reversible increase in voltage across the conductor.

4) If $Q_m < a\tau^2 < Q_m + r\sqrt{\theta_m^2 + 2Q_m(\theta_F - \theta_m) - 2a\tau^2(\theta_F - 1) - a\tau^3}$ (hysteresis region),

Increasing the heat input from $Q_{h1}\Big|_{or}$ causes the voltage to increase. This increase is controllable and reversible up to a heat input of Q_{h1T} (Eq. (13)) at which point $\frac{dV}{dQ_{h1}}$ has become infinite and the voltage increases spontaneously ("take-off") to some finite value. Just before take-off the reduced temperature at the origin $\theta_0 < 1$, thus at the origin the current is shared. Just after take-off $\theta_0 > \theta_F$, thus the region around the origin is completely normal.

If the heat input is increased beyond Q_{h1T} no other take-off is produced, the voltage is again controllable and reversible. If the heat input is decreased from Q_{h1T}, the voltage decreases continuously until the heat reaches Q_{h1R}, at which point the voltage drops spontaneously ("Recovery") to a relatively small value or zero.

Recovery always occurs from a state such that $\theta_0 > \theta_F$ to a state such that $\theta_0 < 1$. According to this model, recovery always occurs before Q_{h1R} is zero.

5) If $a\tau^2 > Q_m + r\sqrt{\theta_m^2 + 2Q_m(\theta_F - \theta_m) - 2a\tau^2(\theta_F - 1) - a\tau^3}$

increasing the heat input from $Q_{h1}\Big|_{or}$ causes the voltage to increase controllably and reversibly until the heat input reaches Q_{h1T}. At this value of heat input the slope $\frac{dV}{dQ_{h1}}$ is infinite and the voltage increases spontaneously to infinity ("quenches"). This region is called the unstable region. Just before take-off $\theta_0 < 1$ so the current is shared at the origin. Note, however, that a "precursor" (a controllable voltage) always appears before the quench.

Typical values of the parameters θ_m, Q_m, θ_f, and r depend upon the applied magnetic field and on the preparation and orientation of the conductor surface. In a superconducting magnet the range of values of these parameters is approximately:

$$.05 < \theta_m < .4$$
$$.05 < Q_m < .3$$
$$.5 < \theta_f < 5$$
$$.1 < r < .3$$

The solutions for the cases $\theta_m > 1 - \tau$ or $\theta_f < 1$ have not been worked out. The solutions, however, ought to contain the same type of behavior as the case we have considered. Some of the equations obtained will of course change; for example, the size of the hysteresis region will be different than that obtained if $\theta_f < 1$.

It is interesting to note that the constant h analysis presented in the 1st QPR also predicts the same kinds of behavior as that obtained from the 2nd heat transfer characteristic. However, numerical values obtained by the constant h analysis are much different than those obtained using the latter model. It is shown in the next section that our new model predicts correctly pertinent experimental quantities.

IV. EXPERIMENTAL RESULTS REGARDING STABILITY CHARACTERISTICS

A. One Dimensional Stability Characteristics

The experimental apparatus was described in Section V of the 2nd QPR. Figure 9 of the 2nd QPR is reproduced here for convenience in discussion as Fig. 7. The figures show the sample voltage V vs heater input current I_h at a constant sample current.

The heat input Q_{h1} is proportional to the heater current squared, thus:

$$\frac{dV}{dQ_{h1}} \sim \frac{dV}{dI_h^2} = \frac{1}{2I_h} \cdot \frac{dV}{dI_h}$$

At the onset of resistance (marked with an x on the figures), we see $\frac{dV}{dI_h} = 0$. But I_h is finite, so we have $\left.\frac{dV}{dQ_{h1}}\right|_{Q_{h1}} = 0$ as predicted. At take-off (Fig. 7b, c, d, marked as point b) $\frac{dV}{dQ_{h1}}$ has become quite large, if not infinite, again as predicted. The reversibility of the voltage after take-off is also illustrated in Fig. 7b, c.

It should be noted that the behavior shown in Fig. 7d is not predicted using the 2nd heat transfer characteristic. Our model predicts that, in the hysteresis region, the sample will be fully superconducting when the heat input is reduced to zero. If the entire sample were normal, the voltage measured would be about 100 millivolts. It is obvious from Fig. 7d that the voltage observed is an order of magnitude too low. Once triggered (by a heat input of Q_{h1T}), a stable normal region exists at this conductor current when the heat input is reduced to zero. It does not propagate nor does it collapse. This behavior, as can be seen from the data, occurs near the end of the hysteresis region. Since this behavior occurs close to the fully unstable region (where quench occurs at take-off), it does not seem profitable, at this time, to use a more detailed heat transfer characteristic to fully determine this behavior.

Quantitative agreement with the theory is also good, considering the uncertainties involved in determining some of the parameters. From Fig. 3, it is seen that h is somewhat undetermined. Also the value of h depends

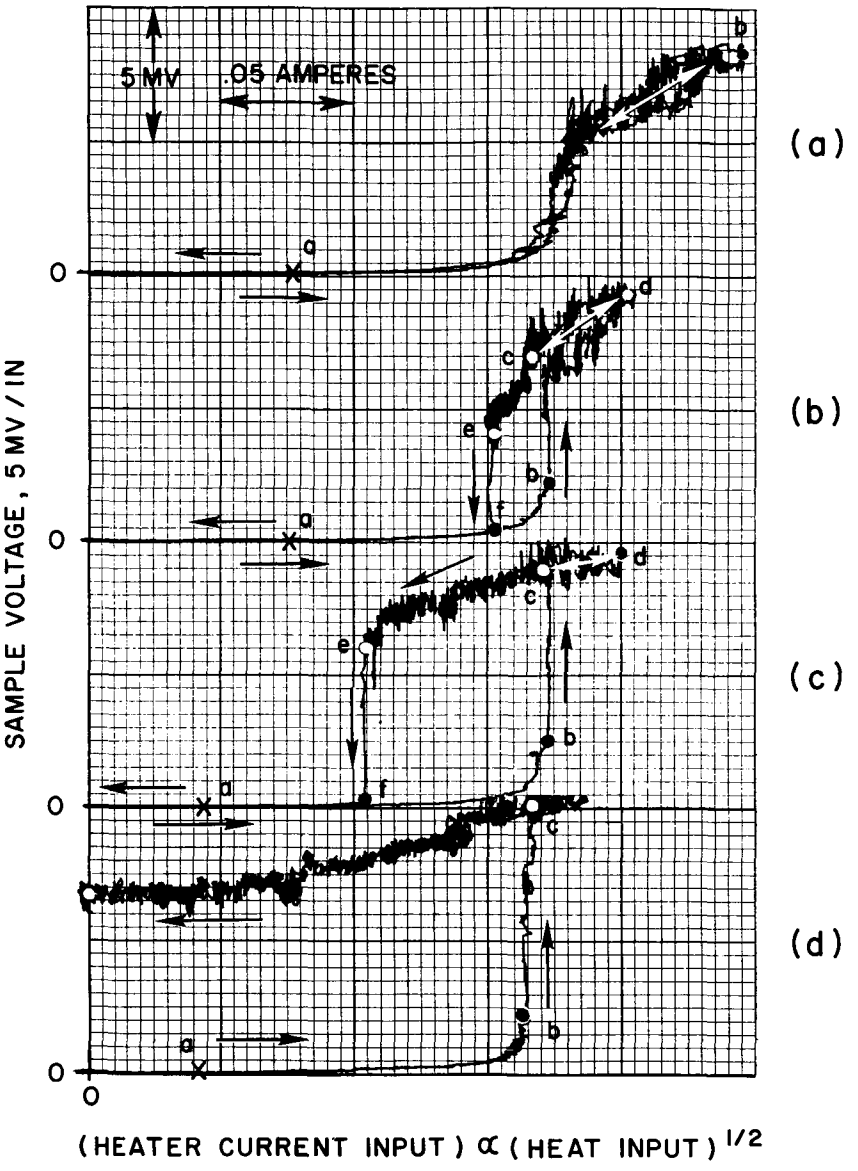

Fig. 7 Typical test results regarding one dimensional stability

a) $I/I_c = .88$, stable operation

b) $I/I_c = .91$, hysteretic behavior

c) $I/I_c = .93$, hysteretic behavior

d) $I/I_c = .94$, unstable operation

on the orientation and preparation of the sample surface. We have chosen a value of $h = 1 \frac{\text{watt}}{\text{cm}^2 - {}^{o}\text{K}}$ as representative -- this may be in error by as much as a factor of 2. The thermal conductivity k, which appears in determining the reduced length ξ and $Q_{h\,1}$, is a function of temperature and copper purity.[4] We chose a value of k = 40 watts/cm - ^{o}K as representative of our sample by extrapolating from the data given by Purcell.[4] It is estimated that this could be in error by as much as 20%. The cooled perimeter P of the conductor is approximately half the total conductor perimeter, as can be seen from the schematic of the experimental setup (Fig. 8 -2nd QPR). It is also estimated that $.15 < \Theta_m < .20$ and $.1 < Q_m < .15$, for this sample at the given applied field (40 kG). In this particular experiment, most of the heat generated by the heater flows into the sample. The heater resistance R is 4.45 ohms.

Using the above values for h and k, and choosing $\Theta_m = .17$, a curve of heater power at the onset of resistance vs $\tau = I/I_c$ may be generated from Eqs. 31 and 32 of the 2nd QPR. Figure 8 shows the comparison between this theoretical curve and the experimental data. This choice of parameters (h = 1, k = 40, $\Theta_m = .18$) fits the data well. However, with the quoted uncertainty in these same parameters, the calculated range of heater power at the onset of resistance is also shown in Fig. 8 by broken lines.

From Fig. 7 it is obvious that the onset of the hysteresis region occurs at about $\tau = .90$. The calculated α for this sample is .175, which could be in error by as much as a factor of 2. Thus, $\alpha \tau^2$ at the beginning of the hysteresis region is approximately (within a factor of two) 0.155. This obviously does not agree with $\alpha \tau^2 = 1$ at the beginning of the hysteresis region as obtained by the constant h solution in the 1st QPR. In fact, the constant h model predicts that for this α there is no hysteresis. This agrees quite well, however, with $\alpha \tau^2 = Q_m$, where Q_m is in the range quoted previously in this report.

It seems that the one-dimensional theory is quite complete. However, further experimental work should be undertaken to determine more precisely the numerical values of the parameters h, k, Θ_m, Q_m. Work has been started on the effect of the helium bath temperature and pressure on the heat transfer properties of the liquid helium (see Section IV-B).

B. Stability Characteristics of a Large Coil

A superconducting coil has been designed, built and tested.* The pertinent coil data is summarized in the following table.

* The design and construction of the coil was performed under a program for NASA-Lewis under contract NAS 3-9684.

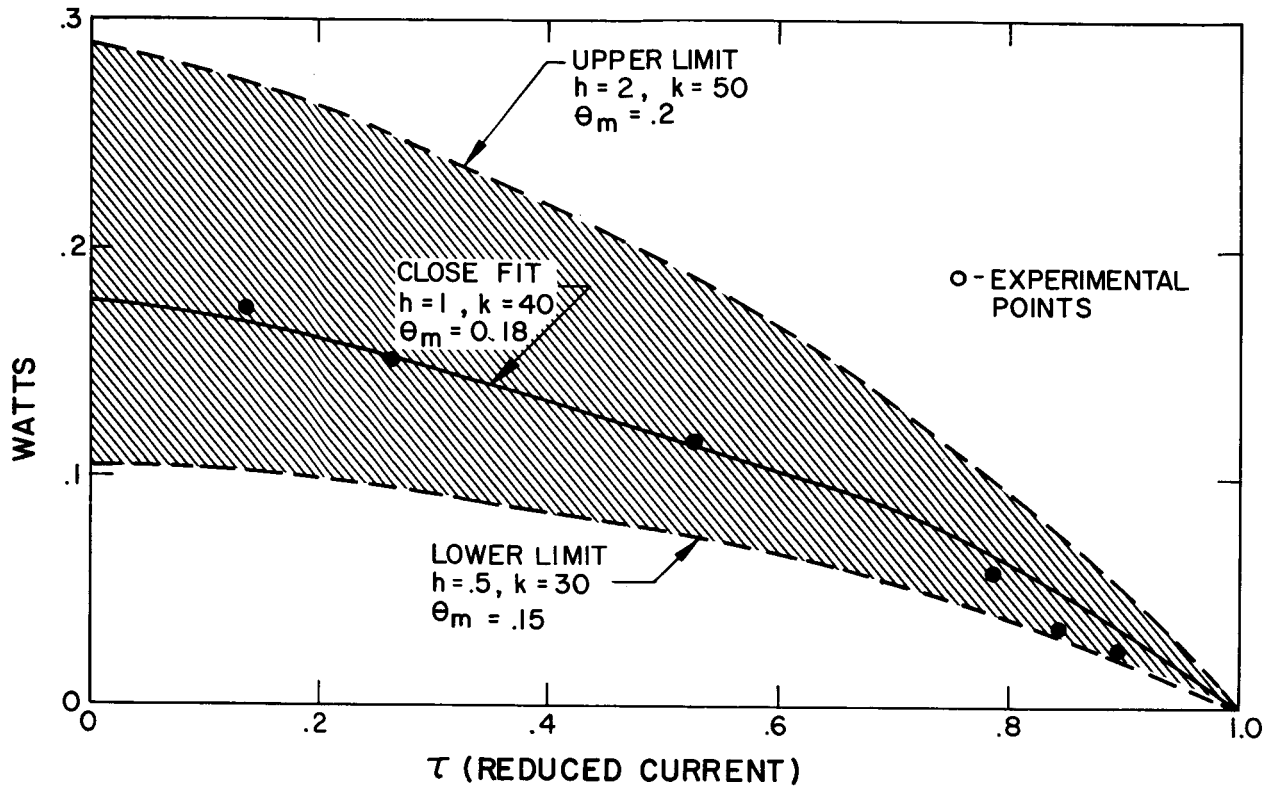

Fig. 8 Heater power at the onset of resistance vs reduced sample current τ

COIL DATA

Winding i.d.	6.030"
Winding o.d.	8.780"
Winding Length	4.00"
Length of Conductor	1136'
Gauss per amp at Center	34.3
Maximum Gauss per amp at Wire	46
Coil Inductance	.052 henries

The conductor is stabilized Niobium-Titanium. There are fifteen .010" NbTi cores in a copper matrix .086" square. The H-I curve for this material is shown in Fig. 9. Figure 10 shows the magnet while being wound. The details of the helium cooling passages can also be seen. Each turn is separated by .006" with intermittent insulation to allow the helium between turns. Each layer (15 layers total) is separated by .015" insulating strips which are spaced to allow the free flow of helium (these are clearly visible in Fig. 10).

The coil is instrumented with four spot heaters at different places in the coil. Only two were used extensively; the field at these heaters as a function of magnet current is shown in Fig. 9. Voltage taps were placed across each of the 15 layers in the coil.

The procedure for testing was the same as that used for the small wire samples previously discussed. The magnet current was held constant; then the heater current was increased from zero and the voltage across the heated section was measured. The data was taken on an X-Y recorder.

Typical heater plots using heater #2 at various currents are shown in Fig. 11. For magnet currents below 570 amperes, the coil develops a reversible voltage as the heat input is increased. At low magnet currents it is obvious that

$$\left.\frac{dV}{dQ_{h1}}\right|_{Q_{h1}}\Big|_{or} = 0$$; however, at high currents it is

impossible to determine the initial slope because of the noise. 570 amperes is the beginning of the hysteresis region. The initial voltage developed before take-off can not be seen because of the noise level. The calculated voltage at take-off V_T (calculated from analysis in 2nd QPR at a magnet current of 600 amperes is 0.40 ± 0.10 millivolts, which is less than the noise level present. Note also in Fig. 11-d that a stable normal region exists, once triggered, when the heat input is reduced to zero at a magnet current of 660 amperes. This same effect has been discussed previously.

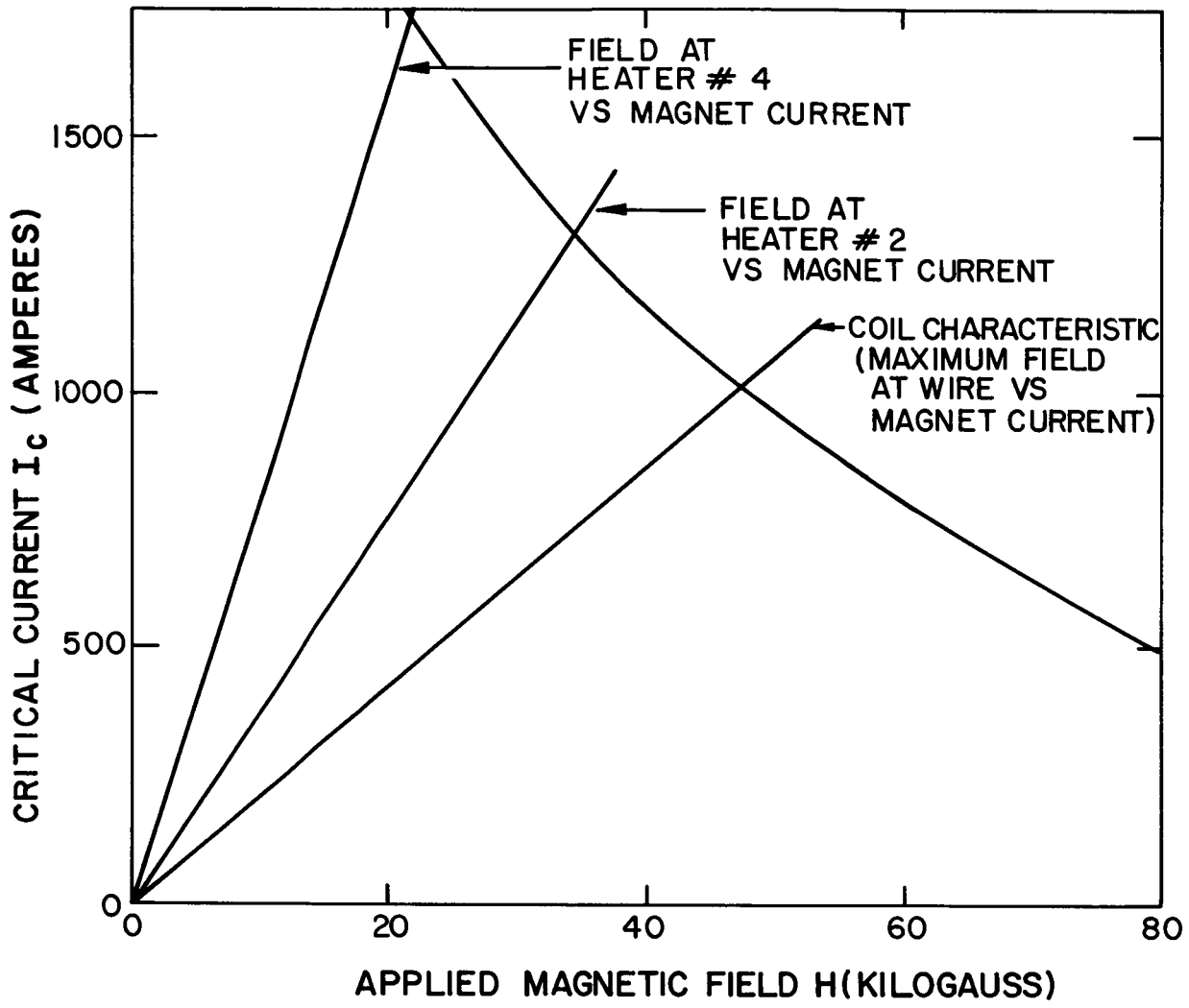

Fig. 9 Short sample H-I characteristic and coil load lines

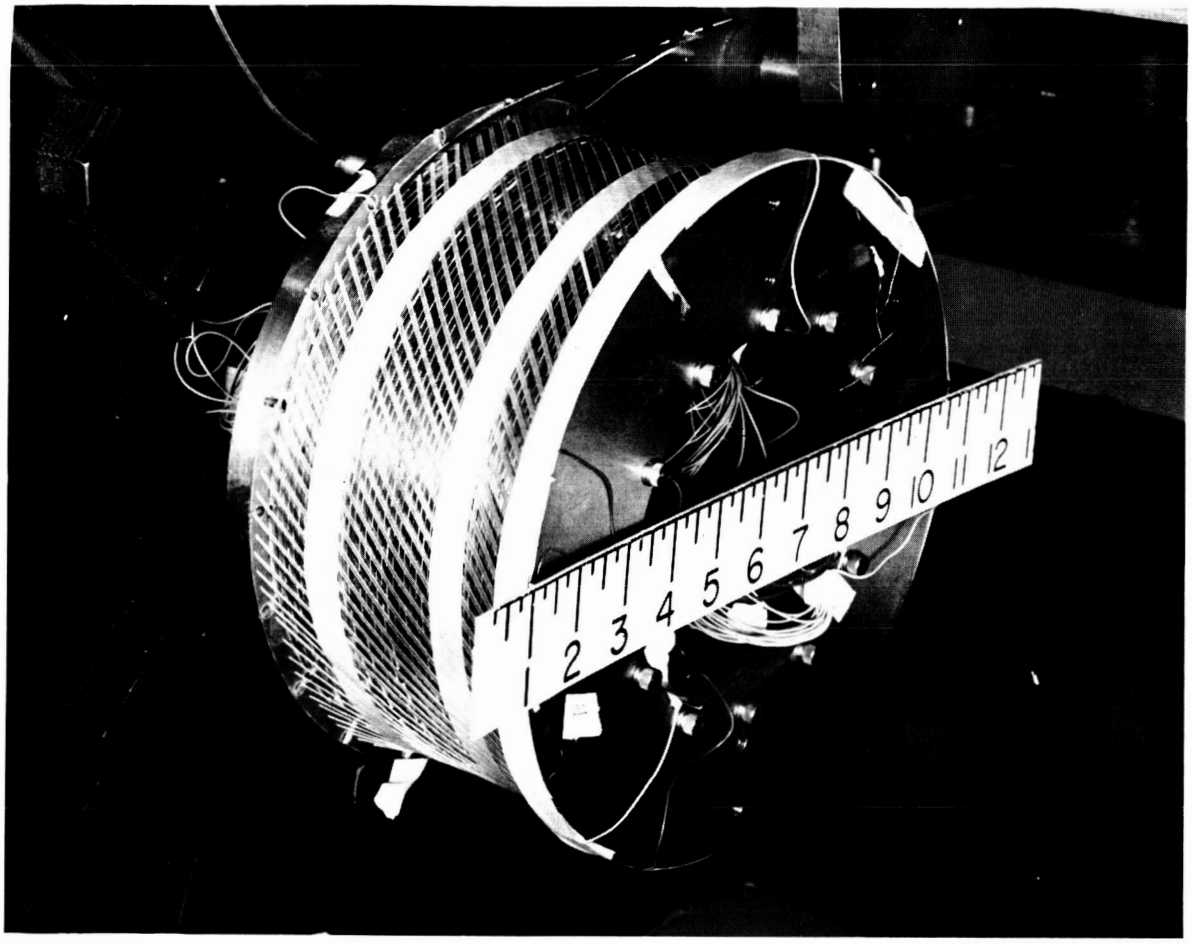

Fig. 10 A view of the magnet being wound

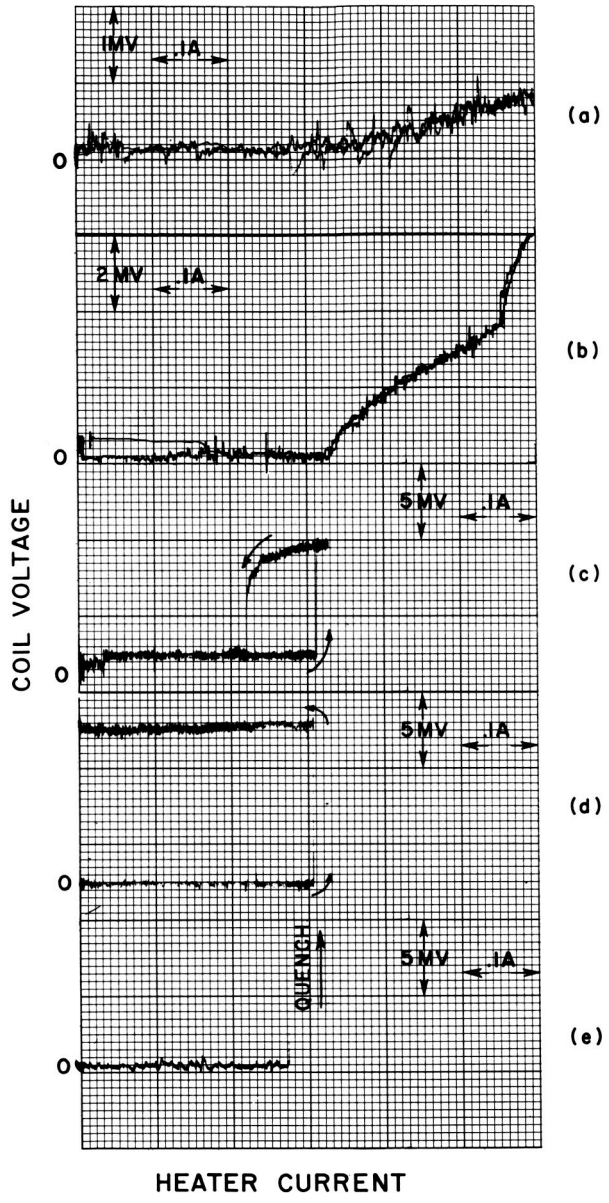

Fig. 11 Typical heater characteristics for the coil shown in Fig. 10 (Htr. #2)

a) At a magnet current of 200 amperes
b) At a magnet current of 500 amperes
c) At a magnet current of 640 amperes
d) At a magnet current of 660 amperes
e) At a magnet current of 800 amperes

The calculated value of α for the conductor near heater #2 at a magnet current of 570 amperes is 1.16. Again, because the value of h is somewhat uncertain, this value of α may be in error by a factor of 2. At the onset of hysteresis, then, $\alpha \tau^2 = .094$, which agrees well with the estimated value of $Q_m \approx .10$.

The heat input at take-off (for currents above 570A) as a function of magnet current is shown in Fig. 12. In comparing the experimental values to those obtained from Eq. 13, it must be remembered that Q_m, Θ_m and α are a function of the magnetic field and thus the magnet current. Also due to the construction of the heaters, not all the heat generated goes into the wire, but some is lost directly to the helium. The theoretical estimates of the heat input at take-off, with the given uncertainties in the parameters, h, Θ_m, Q_m, are also shown in Fig. 12. The value of k was measured for this conductor to be 20 watts/cm-^{o}K within 10% (the method of measurement is discussed in Appendix 1). Again the agreement is good.

So far, the effects discussed have been one dimensional. Two and three dimensional effects began to appear when large amounts of power were being dissipated by the heater and the normal region (about 5 watts). A typical example of a V-Q plot showing 2 dimensional effects is shown in Fig. 13. This plot was taken at a magnet current of 550 amperes, below the one dimensional hysteresis region. As the heat input is increased from zero, a controllable voltage begins to appear at a heater current of $I_h = .33$ ampere. This voltage remains controllable until a heater current of $I_h = .53$ ampere; at this time a jump in coil voltage occurs. The total power dissipated is the heater power plus the power into the magnet -- 6.7 watts. This discontinuous rise occurs when the normal spot jumps into the next turn in the same layer of the magnet. Another jump occurs soon thereafter. These are two dimensional effects. The adjacent layers in the magnet did not develop a voltage even though the maximum power dissipated was 14.5 watts (after the 2nd jump). Upon reducing the heater current, both adjacent turns recovered at the same time. When the heater current was increased to $I_h = .65$ ampere (not shown in Fig. 13), a voltage began to appear across the inner adjacent layer and the magnet quenched. This behavior was typical of a quench; the normal region propagated to an adjacent layer just before quench. Then the normal region transfered to an adjacent layer; the helium passages became vapor bound causing the quench to occur. Even though the one dimensional theory predicts that the V-Q plot at this magnet current should be completely continuous and reversible, hysteresis and quench can be caused to occur if the heat inputs are large enough, but these effects are two and three dimensional. For this particular design of helium cooling passages, one dimensional effects always occurred before two or three dimensional effects.

Another interesting phenomina was observed with this coil; the quench current (with zero heater power) depended upon the charge rate. This coil did not develop a controllable voltage after the critical current was reached even at slow charge rates because the coil was not strictly stable ($\alpha \approx 1$ for the innermost turns at critical current). Figure 14 shows

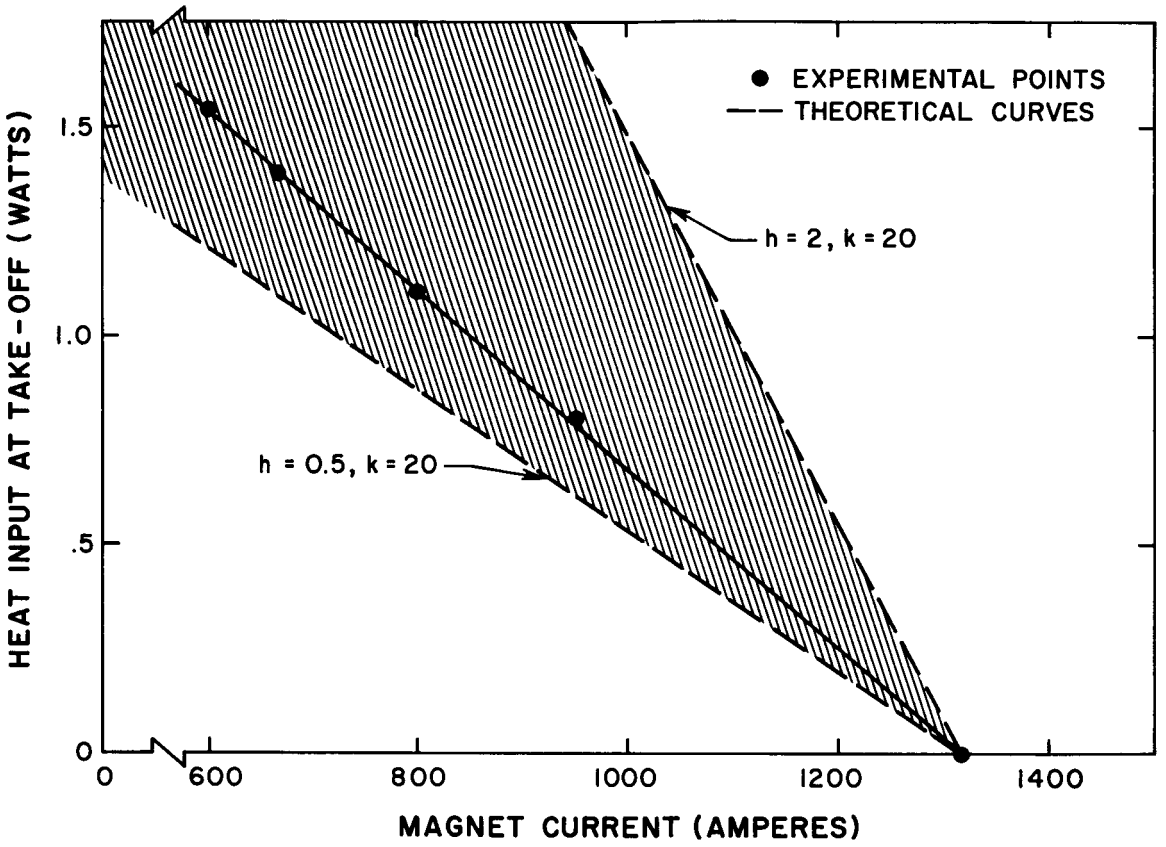

Fig. 12 Heat input at take-off vs magnet current

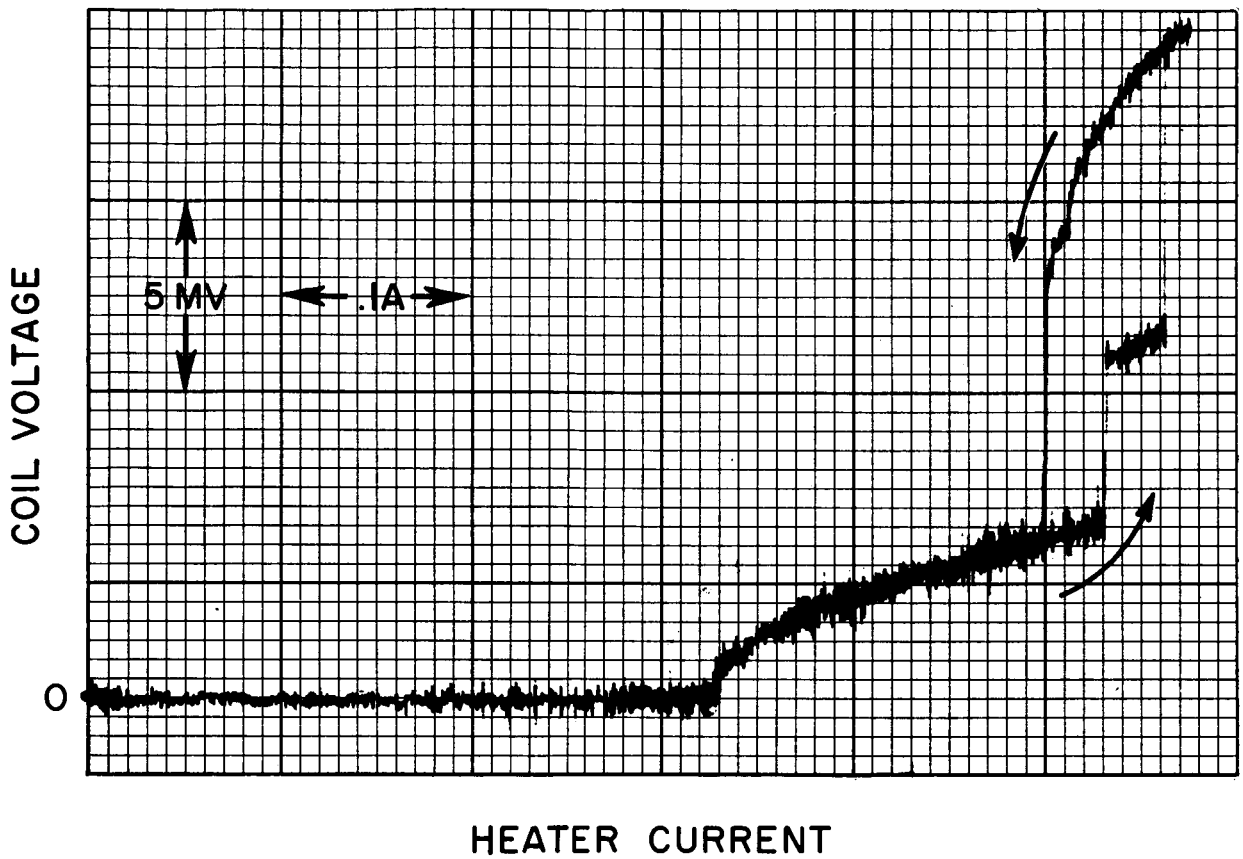

Fig. 13 A heater plot showing typical two dimensional behavior at a magnet current of 550 amperes

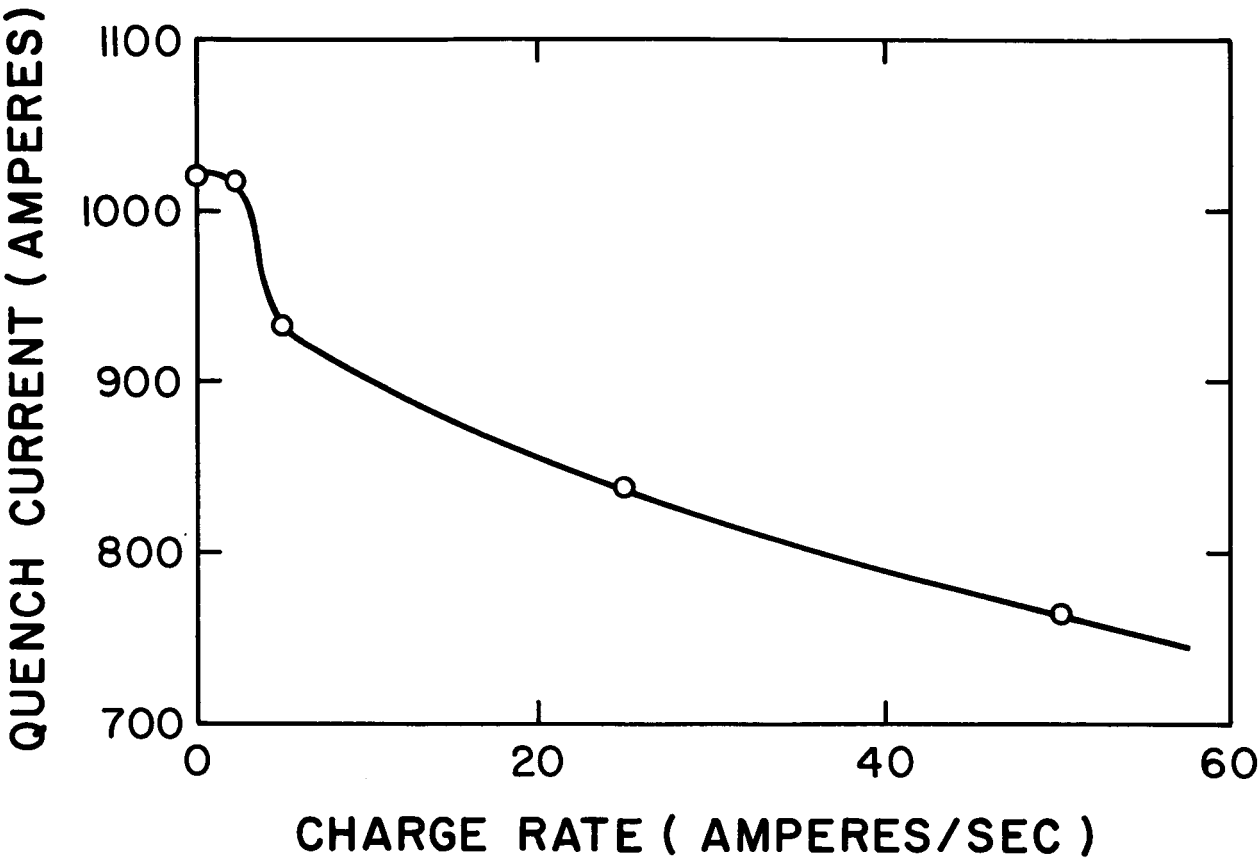

Fig. 14 Quench current vs charge rate for the coil

the quench current vs charge rate. At low charge rates, the short sample critical current was always reached. Heating occurs in the coil during the charge because of the AC resistance of the superconductor and eddy current losses in the copper. In fact at any charge rate, the helium could be seen to boil -- and at the highest rate (50 A/sec) the boiling was so vigorous that the coil could not be seen through all the bubbles. Below a magnet current of 600 A, the coil could not be quenched even at a charge rate of 100 A/sec (maximum rate available from the current supply used.)

C. Effect of Pressure and Temperature of the Helium Bath on the Stability of the Coil

The dewar used for the previous experiment on the coil could be pressurized to 30 lbs/sq in. or it could be pumped in with a large vacuum pump to reduce the bath temperature. Experiments were completed both under pressure and at temperatures below 4.2°K.

The easiest way to present the effects of pressure on the stability of the coil is to choose a magnet current in the hysteresis region at atmospheric pressure; then, holding this current constant, V-Q plots are taken at different pressures. Since the pressurization of the dewar is an adiabatic process, the temperature of the liquid (when below the critical pressure) remains constant. Above the critical pressure, there is a slight increase in temperature ($\approx 0.1^{\circ}K$) because the entropy of the helium must remain constant. Thus we assume that the temperature of the helium remains 4.2°K at any pressure above atmospheric. If under pressure the hysteresis loop becomes larger at a constant magnet current the stability is becoming worse; if it becomes smaller, the stability is getting better. As mentioned previously, these effects, at low heater powers, are one dimensional only. A typical example of the results is shown in Fig. 15, where the heater current at take-off and the heater current at recovery are plotted vs the dewar pressure (in pounds pressure gauge). The critical pressure of Helium is 18.5 lbs/sq in. As can be seen, the stability of the coil decreases until the critical pressure is reached. Beyond the critical pressure, the coil is about as stable as at atmospheric pressure, and the stability seems to be independent of the pressure.

Above the critical pressure boiling does not occur, convection and conduction are the only mechanisms by which cooling can occur. The heat transfer properties of the helium are now better approximated by the constant h characteristic presented in the 1st QPR. However, the value of h is much smaller than at atmospheric pressure. Thus, even though the beginning of the hysteresis region is given by $\alpha \tau^2 = 1$ above the critical pressure (1st QPR), the value of α has increased because α is proportional to 1/h. The net effect, as can be seen from Fig. 15, is that there is no increase in stability at pressures greater than the critical pressure.

The temperature of the liquid helium is easily reduced by pumping on the helium gas above the liquid with a large vacuum pump. The testing procedure was the same as that used for the pressure tests. A magnet

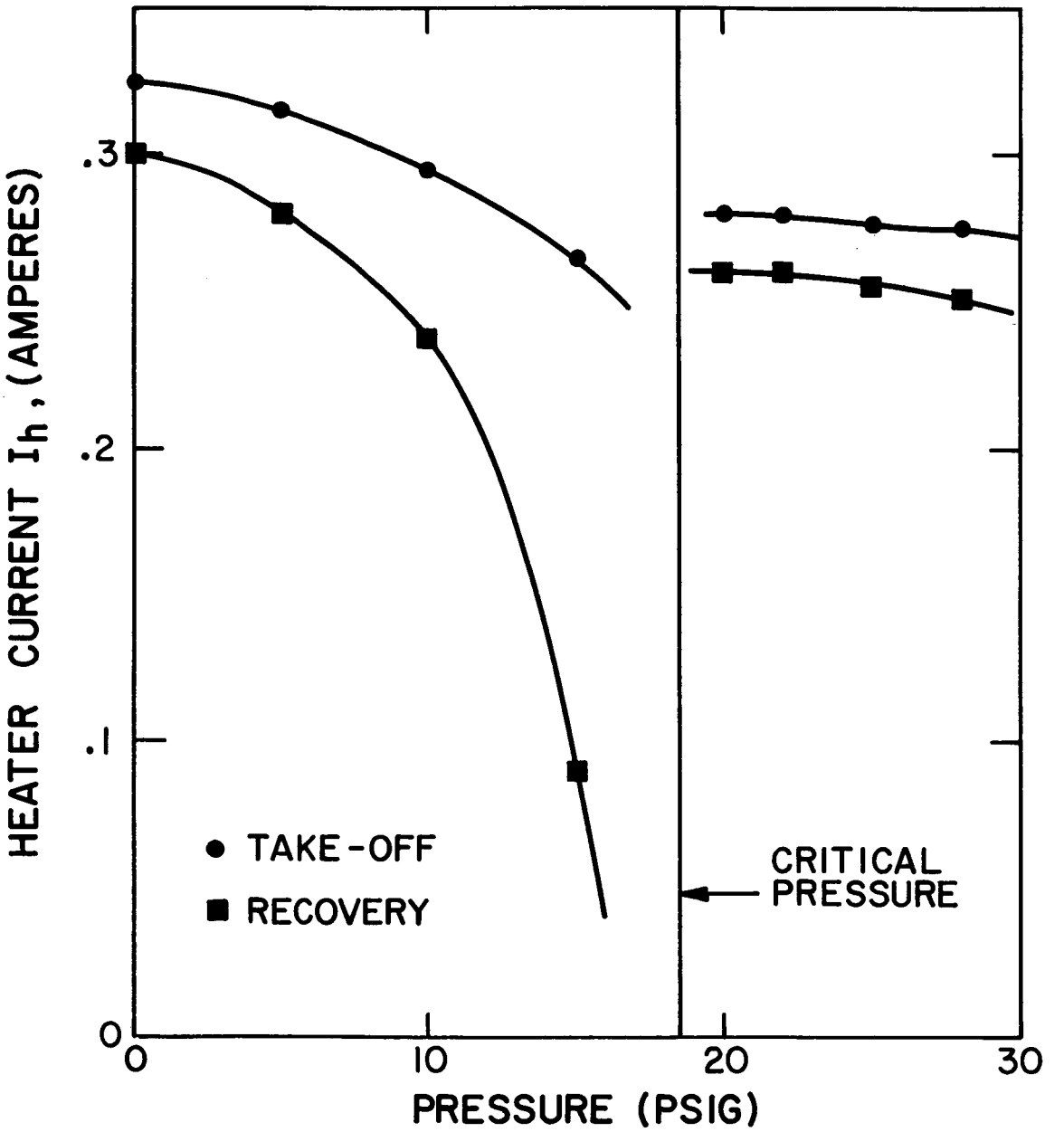

Fig. 15 Heater current at take-off and recovery vs helium pressure at a magnet current of 620 amperes

current of 600 A was used and V-Q plots were taken at different temperatures. The temperature of the liquid was determined by using a calibrated carbon thermometer and also by observing directly the pressure of the helium gas in the dewar.

It should be remembered that reducing the bath temperature increases the critical current. The critical current at the bath temperature with a constant applied magnetic field H is well approximated by:

$$I_c\ (T_B,\ H) = I_o\ (H)\left[1 - \frac{T_B}{T_c\ (H)}\right] \tag{39}$$

where $I_o\ (H)$ = Critical current at the applied field at zero degrees

$T_c\ (H)$ = Critical temperature at the applied field and zero current

Also the parameters h, Θ_m, Q_m are expected to be a function of the bath temperature T_B · Q_m was defined in the 2nd QPR to be:

$$Q_m = \frac{q_m}{h\left[T_c\ (H) - T_B\right]}$$

where q_m = critical heat flux per unit area when $\Theta_m < \Theta < \Theta_F$.

Using Eq. 39 and the definition of α (1st QPR), $\alpha \tau^2$ as a function of temperature at a magnet current I is:

$$\alpha \tau^2 = \frac{\rho I^2}{h\ P\ A\left[T_c\ (H) - T_B\right]} \tag{40}$$

ρ is independent of temperature below about 10°K for our conductor.[5] The beginning of the hysteresis region is given by Eq. 33:

$$\alpha \tau^2 = Q_m \qquad \text{or} \qquad \frac{\rho I^2}{A} = P q_m \tag{41}$$

Some experimental measurements of q_m as a function of temperature have been reported by Lyon.[6] He finds that below 4.2°K the value of q_m decreases with decreasing temperature until the λ point is reached. Below the λ point q_m becomes much larger than that at 4.2°.

The results of the experiments at reduced temperatures at a constant magnet current (I = 600 amperes) are summarized in Fig. 16. In this figure the heater current at take-off and recovery is shown at different helium temperatures. It is obvious that the stability decreases slightly as the temperature is reduced until the λ point is reached. This agrees with Lyon's observations that q_m decreases as the temperature is decreased. However, below the λ point, the operation at 600 A is no longer hysteretic. Again, this agrees with Lyon's observation that q_m increases rapidly below the λ point. The V-Q plot taken at T = 2.96°K is shown along with that taken at T = 2°K (below λ point, T_λ = 2.18°K) in Fig. 17.

Further reduction in temperature could not be obtained with this experimental setup, because the vacuum pump did not have the capacity. Also at 2°K the magnet current could not be increased above 600 A (to determine the onset of hysteresis) because the current leads became too hot. It appears that there is a gain in stability by operating below the λ point and further experimental work in this area is now being planned.

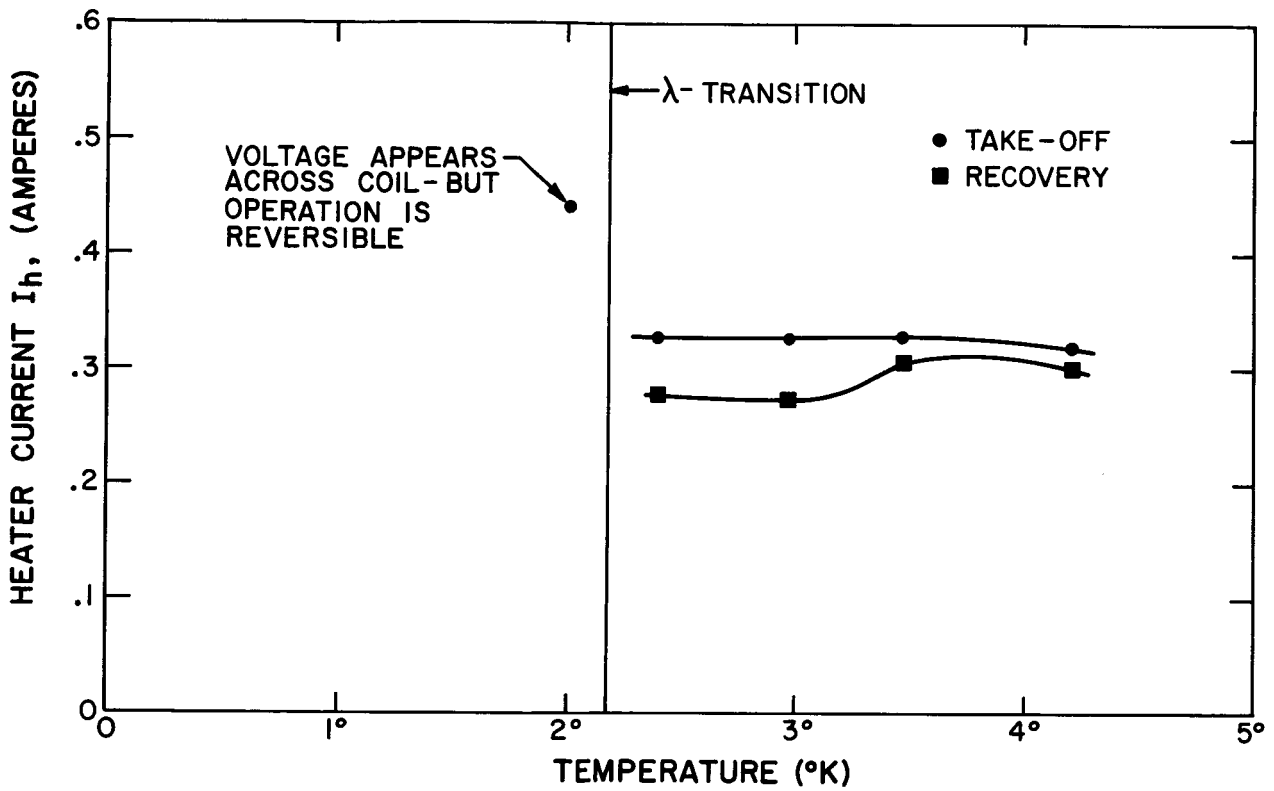

Fig. 16 Heater current at take-off and recovery vs bath temperature at a magnet current of 620 amperes

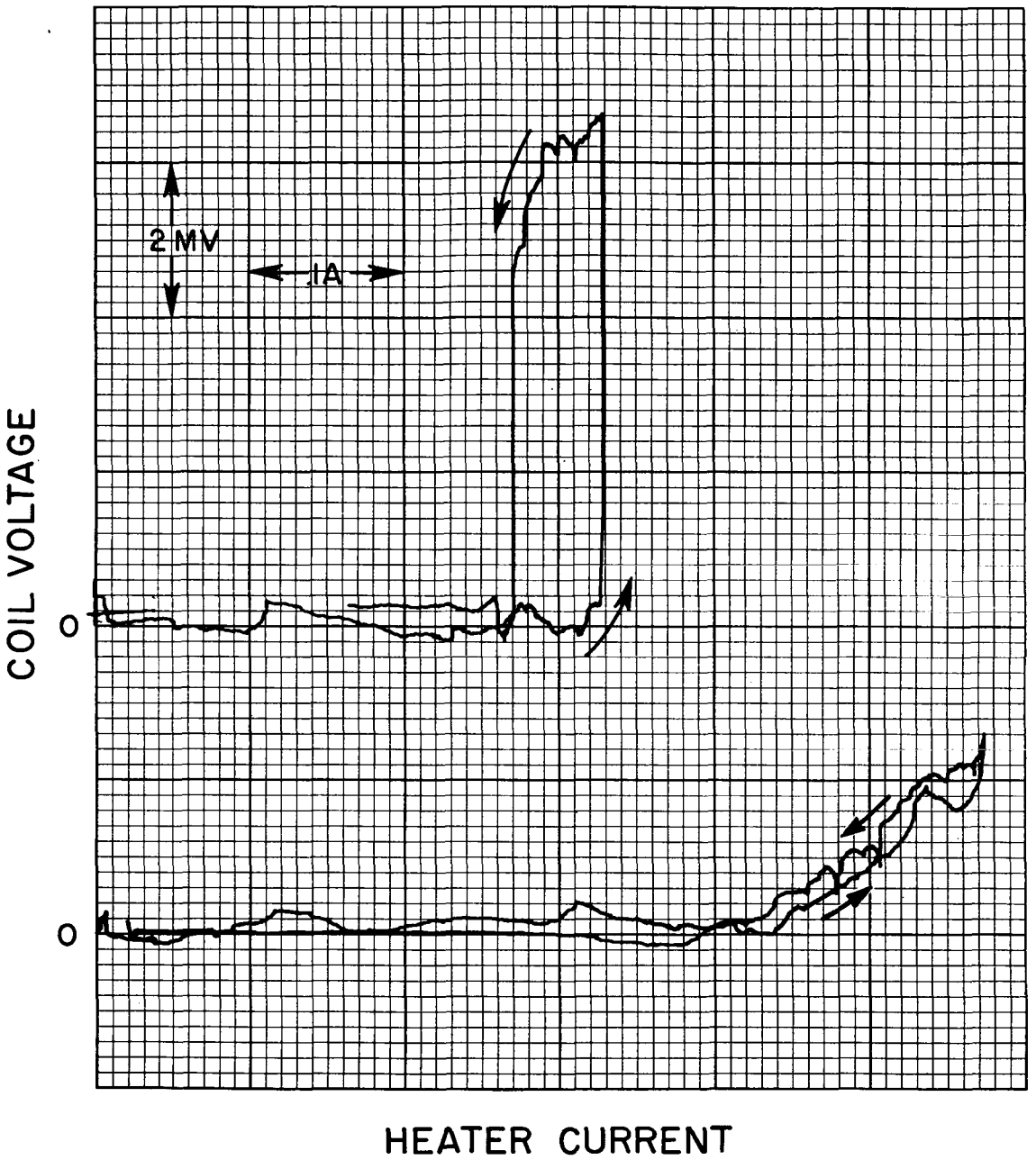

Fig. 17 Typical heater characteristics above and below the λ point at a magnet current of 600 amperes

a) Bath temperature = 2.96°K

b) Bath temperature = 2.0°K

A8741

V. EFFECT OF A GRADUAL RESISTANCE RISE IN THE SUPERCONDUCTOR AT CURRENTS GREATER THAN THE CRITICAL CURRENT

The previous analysis assumed that the superconductor current is just the critical current of the superconductor at the composite conductor temperature. The resistivity of the superconductor at constant applied magnetic field and temperature is then a function of superconductor current as shown in Fig. 18-A. For currents below the critical current, the resistivity is zero, at the critical current the resistivity rises with an infinite slope. Recent experimental evidence[2] indicates that the resistivity increases approximately linearally with current above the critical current as shown in Fig. 18-B. We shall now derive the zero dimensional terminal characteristics of a composite conductor with this new superconductor characteristic.

The superconductor resistivity at currents above the ciritical current at the applied magnetic field and composite temperature is given by

$$\rho_s = k\,(I'_s - I_s) \tag{42}$$

where I'_s = actual superconductor current

I_s = superconductor critical current at the composite temperature and applied magnetic field

k = slope of resistivity increase-to be experimentally determined

ρ_s = superconductor resistivity

It is expected that as $k \to \infty$, the previous results will be reproduced.

The voltage per unit length must be the same in the superconductor and substrate since they are in parallel, thus:

$$\frac{k}{A_s}\left[(1-f)\,I - I_s\right] = \frac{\rho}{A}\,\frac{f}{1-f} \tag{43}$$

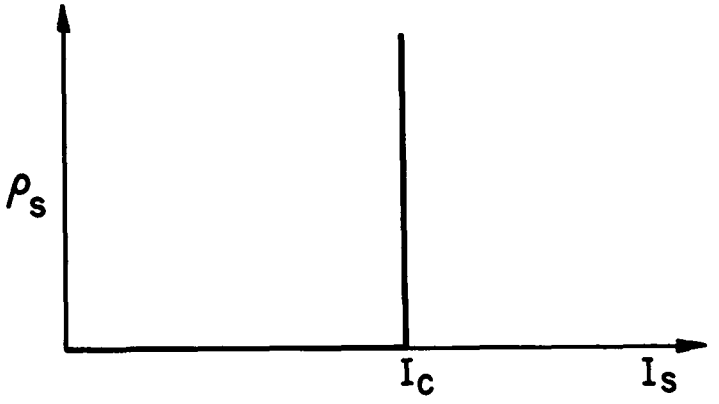

A. ASSUMED RESISTIVITY OF THE SUPERCONDUCTOR ρ_s vs THE SUPERCONDUCTOR CURRENT I_s.

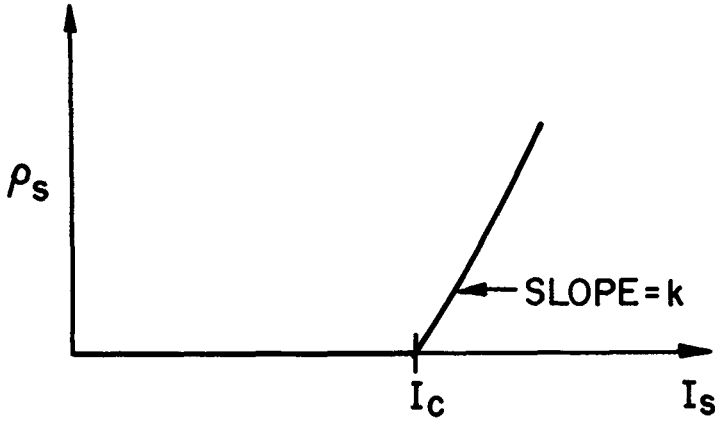

B. EXPERIMENTAL MEASUREMENT OF THE RESISTIVITY OF THE SUPERCONDUCTOR ρ_s vs THE SUPERCONDUCTOR CURRENT I_s.

Fig. 18 Models for the resistivity of the superconductor as a function of the superconductor current

where

As = cross-sectional area of superconductor

A = cross-sectional area of a substrate

I = total composite current

ρ = resistivity of substrate

f = fraction of current in the substrate

We assume that the variation of the superconductor critical current I_s with temperature can be approximated by a linear relationship as before (Eq.(1)-- 1st QPR):

$$I_s = I_c \left(1 - \frac{T_s - T_b}{T_c - T_b}\right) \tag{44}$$

The heat produced in the sample due to joule losses must be transferred to the helium bath. If we assume a constant heat transfer coefficient h for the helium we have:

$$\frac{\rho}{A} I^2 f = h P (T_s - T_B) \tag{45}$$

where the parameters h, P have been defined in the 1st QPR . When Eqs. (41) and (42) are substituted into Eq. (40), Eq. (40) becomes:

$$\alpha f \tau^2 + (1-f) \tau - \left(1 + \frac{\gamma f}{1-f}\right) = 0 \tag{46}$$

where α, τ have been defined previously in the 1st QPR and

$$\gamma = \frac{\rho A_s}{kAI_c} \tag{47}$$

To determine the effect of the gradual rise in superconductor resistance, we determine the rate of voltage increase with current at $\tau = 1$ and $f = 0$.

When the voltage first appears, the current is just beginning to exceed the critical current, and the superconductor resistance is "small". At this point, then, the effect of the gradual rise in resistance is most pronounced. We have:

$$\left.\frac{d\left(\frac{vA}{\rho I_c}\right)}{d\tau}\right|_{\substack{\tau = 1 \\ f = 0}} = \left.\frac{df}{d\tau}\right|_{\substack{\tau = 1 \\ f = 0}} = \frac{1}{1 + \gamma - \alpha} \qquad (48)$$

where v is the voltage per unit length. From our earlier model we would have obtained[7]:

$$\left.\frac{df}{d\tau}\right|_{\substack{\tau = 1 \\ f = 0}} = \frac{1}{1-\alpha}$$

Unless γ is comparable to unity the effect of a gradual resistance increase with current above the short sample current carrying capacity can be neglected, and the results using the former model are sufficient for calculating purposes.

An experiment was carried out in order to estimate the value of γ. A short sample of composite superconductor was placed in a uniform magnetic field so that the current flow was perpendicular to the field. The sample had a large amount of copper substrate on it so that the value of α could be made small. The sample voltage-current characteristic was obtained on an X-Y recorder at applied magnetic fields up to 50 kG and the initial slope $\left(\frac{dv}{dI}\right)$ at the onset of voltage was measured.

The value of the ρ for the copper is obtained by using the fact that ρ is independent of temperature below about $10^{\circ}K$[5]. The sample was placed in a calorimeter and the sample temperature was increased above the transition temperature of the Nb-Ti ($T_c \approx 9.4^{\circ}K$). The resistance of the composite was then measured. The resistance of the Nb-Ti could be neglected because it is very large in the normal state.

The value of γ could only be given an upper limit because of the large uncertainity in the value of α. We found from the above measurements that:

$$0 \leq \gamma \leq .25$$

The value of γ could be increased by either increasing A_s or decreasing A. However, this would only increase the value of α at least as fast as γ increases. Also, if a "reasonable" degree of stability is desired, then the cross sectional area of the copper will be the same order of magnitude as the superconductor cross section. Thus γ will be small compared to unity for most composite superconductors, and the effect of the gradual increase in resistance can be neglected. We expect that our former model of the superconductor will predict correct results, because it is a close approximation to the observed characteristics. Indeed, we see from Section IV that the experimental results agree well with those predicted by our previous model. We will in the future continue to use our former model of the superconductor.

VI. DISCUSSION

In the last three quarters much time has been spent developing stability criteria for composite conductors. The method has always been to consider the effect of an external disturbance, a steady state heat input. We have shown experimentally that, if the cooling is good in a magnet, one dimensional effects determine the onset of resistance. Also, except at large power dissipations, one dimensional effects determine the stability criterion. That is, at large magnet currents (above 550 A in our experiment), take-off occurs from one dimensional effects.

It is obvious from the experiment on the large coil that a magnet can operate in a region that is "unstable." We have defined "complete stability" by the condition that $\alpha \tau^2 < Q_m$. If the magnet current is such that $\alpha \tau^2 > Q_m$ at any point in the coil, then this part of the coil is in the hysteresis or unstable region. Using the V-Q plots, it was determined that the end of the "stable" region was at a magnet current of 570 amperes. At currents above 570 amperes the magnet was in the unstable region. Yet, the magnet could be charged to the short sample characteristic (at low charging rates). The obvious conclusion is that the natural disturbances present in the magnet (flux jumps) are not as large as the external disturbance (heat input) that causes instability ($Q_{h\,l\,T}$).

The "amount of stability" needed in a particular magnet is determined by several factors: the magnitude of the internal disturbances (flux jumps), the magnitude of external disturbances such as vibration or heat inputs, and the particular use of the magnet. If a magnet is to be used to generate a steady state magnetic field, and there are no external disturbances, and an accidental quench (say by exceeding the design current) will not harm the magnet, then stability against flux jumps is all that is needed. We will call this stability "transient stability". If, however, the magnet is to be used on a transient basis (say to discharge into a load in a short time), the coil must be completely stable. (A large coil for such a purpose has been designed, built and successfully operated by Avco)[8]. There are a variety of applications of magnets for which stability between these two limits is needed. It is obvious that "transient stability" is a less rigid stability criteria than "complete stability".

Work is going to be continued to determine the effects of operation below the λ point, in particular the extension of the complete stability region. Theoretical and experimental studies of "transient stability" are also expected to be started next quarter.

REFERENCES

1. 2nd Quarterly Progress Report

2. Dissipative Mechanism in Type II Superconductors -- Y. B. Kim et al Phys. Rev. Letts., Vol. 13, #26, December, 1964.

3. 1st Quarterly Progress Report

4. WADD Technical Report 60-56 Part II -- A compendium of the properties of materials at low temperatures (Phase I) part II.

5. WADD Technical Report 60-56 Part IV -- A compendium of the properties of materials at low temperatures (Phase II) Part IV.

6. Boiling Heat Transfer and Peak Nucleate Boiling Fluxes in Saturated Liquid Helium Between the λ point and the Critical Temperature -- D. N. Lyon -- International Advances in Cryogenic Engineering, Vol. 10 -- 1964.

7. Experimental Investigation of Advanced Superconducting Magnets -- Ethan Hoag et al -- Final Report NAS 8-5279, January, 1967, pg. II - 15

8. The use of Superconducting Coils as Energy Storage Elements in Pulsed System Operations -- E. J. Lucas, et al -- Paper delivered at IEEE Intermagnetics Conference April, 1967 to be published by IEEE.

APPENDIX I

The average value of the thermal conductivity of annealed OFHC copper (99.99% pure) has been measured. The method of measurement is to immerse one end of the sample in liquid helium, heat the other end and measure the temperature at the heated end. A schematic of the experimental setup is shown in Fig. A-1. The sample was the previously described Avco stabilized composite conductor .086" square. The copper matrix has a thermal conductivity several orders of magnitude larger than the Nb–Ti so the thermal conduction is due completely to the copper. A calibrated carbon thermometer is used to measure the temperature. The entire sample is insulated with mylar tape down to the liquid helium level, so that the heat flow is one dimensional.

The average thermal conductivity k is determined from the following equation:

$$k = \frac{qL}{\Delta T A}$$

where

q = heat input from heater

L = distance from heater to the liquid helium bath

ΔT = Temperature of conductor at the heater minus the bath temperature (4.2°K)

A = cross sectional area of the copper

For this sample L = 10 cm, $A = 3.5 \times 10^{-2}$ cm^2. The value of k obtained is (perhaps 10%) in error, because the temperature of the conductor at the helium level is slightly higher than 4.2°K when the heater is on. The thermal conductivity of pure copper rises as the temperature is increased up to 15°K.[4] Thus we expect that the average thermal conductivity will rise with ΔT (up to $\Delta T = 10^{\circ}K$). The measured value of k (average thermal conductivity) vs. ΔT is shown in Fig. A-2.

The value of $k = 20 \frac{\text{watts}}{\text{cm} - {}^{0}K}$ was chosen for the calculation of q_T for the coil discussed in part IV-B because the ΔT was small. These values of k agree well with the extrapolated values obtained from the data by Purcell.[4]

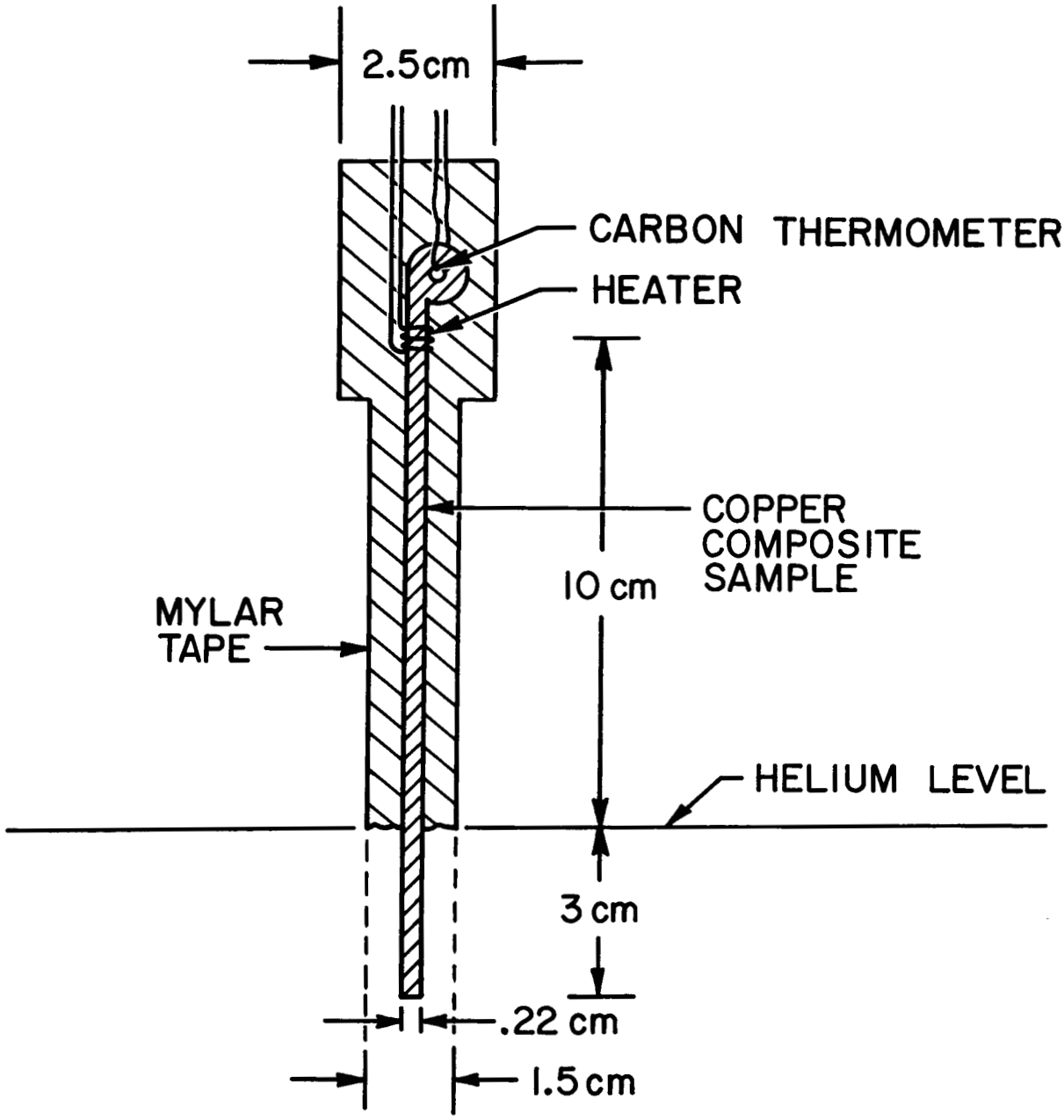

Fig. A-1 Experimental setup to determine the average thermal conductivity of copper

A8743

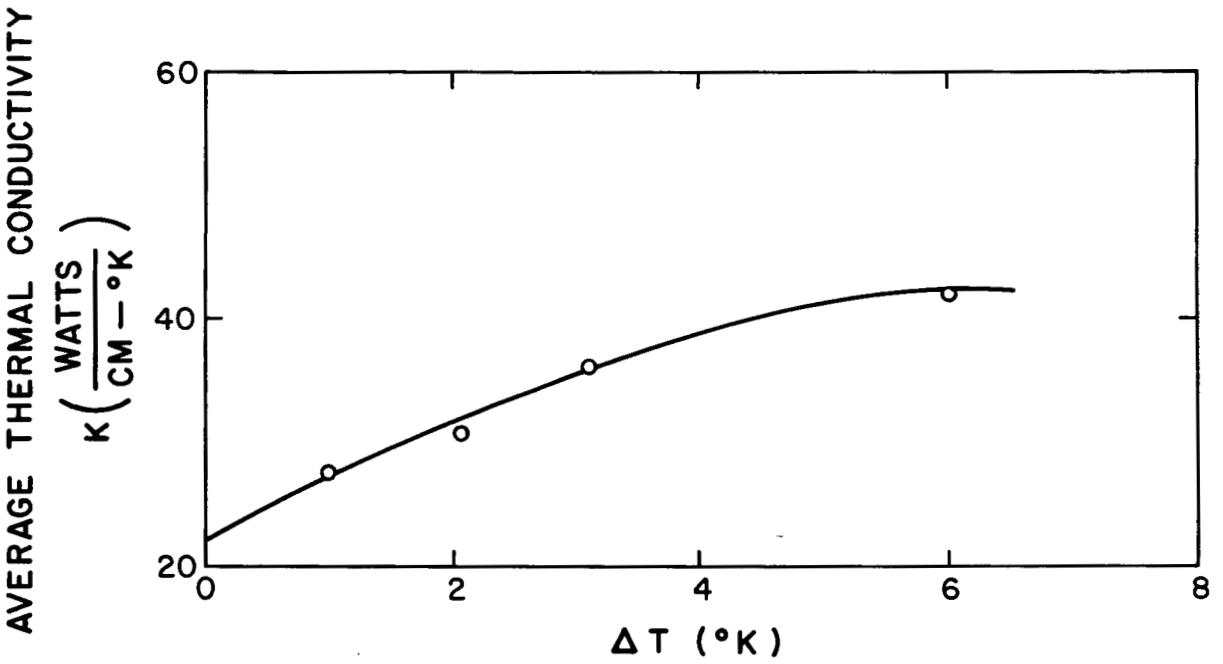

Fig. A-2 Measured average thermal conductivity vs ΔT

ERRATA

In the 1st QPR Eq. (20) should be replaced by:

$$\tau_R = \left(\frac{I}{I_c}\right)_R = \frac{(a - a_i) \pm 2\sqrt{-a\, a_i + a_i\,(a + a_i)^2}}{(a + a_i)^2}$$

$$\text{IF} \quad \frac{a - \sqrt{a}}{a_i} < 1 \quad ;$$

$$\text{BUT IF} \quad \frac{a - \sqrt{a}}{a_i} > 1 \qquad \text{then}$$

$$\tau_R = \frac{1}{\sqrt{a}} \quad \text{independent of} \quad a_i$$

Equation (21) of the 1st QPR should be replaced by

$$f_R = \sqrt{\frac{1 - \tau_R}{a_i\ \tau_R^2}} \quad \text{IF} \quad \frac{a - \sqrt{a}}{a_i} < 1 \quad ;$$

$$\text{BUT IF} \quad \frac{a - \sqrt{a}}{a_i} > 1 \quad , \quad f_R = 1$$

Consequently Fig. 2 of the 1st QPR should be replaced by Fig. E-1 shown here. Note that, above the line given by $\frac{a - \sqrt{a}}{a_i} = 1$, $V_R = \tau_R$ since $f_R = 1$.

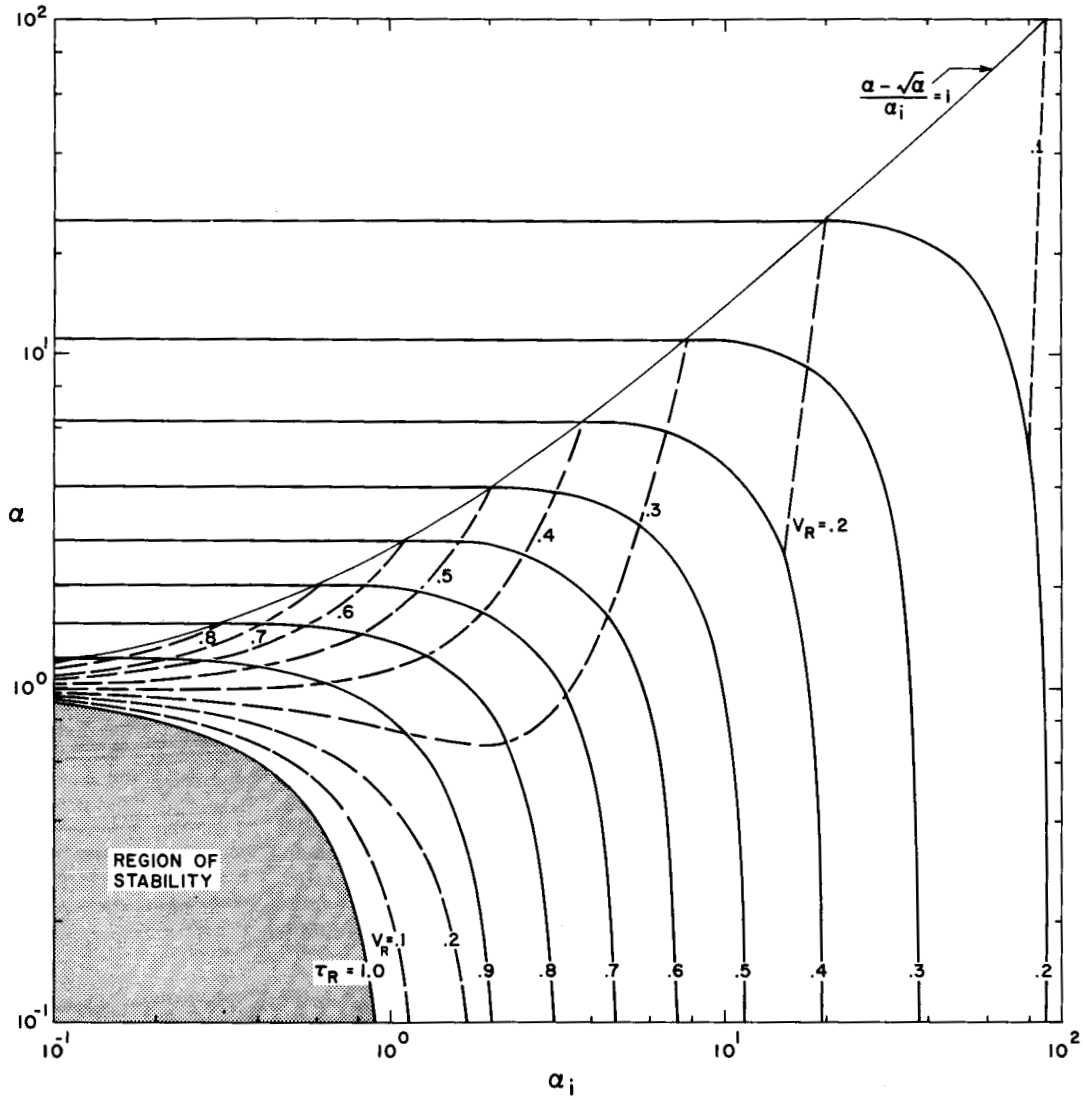

Fig. E-1 Recovery current τ_r and recovery voltage V_r as a function of α and α_i

A7459